DISTRIBUTION STATEMENT A
Approved for Public Release
Distribution Unlimited

Final Proceedings of The EOARD/IRC-sponsored International Workshop on Gamma Aluminide Alloy Technology

held from 1 to 3 May 1996
at The IRC in Materials for High Performance Applications
The University of Birmingham

SECTION TWO

The organisers wish to thank the United States Air Force European Office of Aerospace Research and Development for its contributions to the success of this conference

DTIC QUALITY INSPECTED 1

20000223 172

Interdisciplinary Research Centre

in

Materials for High Performance Applications

Final Proceedings of
The EOARD/IRC-sponsored
International Workshop on Gamma
Aluminide Alloy Technology

held from 1 to 3 May 1996
at The IRC in Materials for High Performance
Applications
The University of Birmingham

SECTION TWO

Reproduced From
Best Available Copy

THE UNIVERSITY
OF BIRMINGHAM

UNIVERSITY OF WALES
SWANSEA

THE UNIVERSITY OF BIRMINGHAM AND UNIVERSITY OF WALES SWANSEA CONSORTIUM

Funded by the Engineering and Physical Sciences Research Council

AQF00-05-1327

REPORT DOCUMENTATION PAGE

Form Approved OMB No. 0704-0188

Public reporting burden for this collection of information is estimated to average 1 hour per response, including the time for reviewing instructions, searching existing data sources, gathering and maintaining the data needed, and completing and reviewing the collection of information. Send comments regarding this burden estimate or any other aspect of this collection of information, including suggestions for reducing this burden to Washington Headquarters Services, Directorate for Information Operations and Reports, 1215 Jefferson Davis Highway, Suite 1204, Arlington, VA 22202-4302, and to the Office of Management and Budget, Paperwork Reduction Project (0704-0188), Washington, DC 20503.

1. AGENCY USE ONLY (Leave blank)	2. REPORT DATE	3. REPORT TYPE AND DATES COVERED
	18 April 1997	Conference Proceedings

4. TITLE AND SUBTITLE	5. FUNDING NUMBERS
International Workshop on Gamma Aluminide Alloy Technology	F6170896W0160
6. AUTHOR(S) Conference Committee	
7. PERFORMING ORGANIZATION NAME(S) AND ADDRESS(ES) University of Birmingham Edgbaston Birmingham B15 2TT United Kingdom	8. PERFORMING ORGANIZATION REPORT NUMBER N/A
9. SPONSORING/MONITORING AGENCY NAME(S) AND ADDRESS(ES) EOARD PSC 802 BOX 14 FPO 09499-0200	10. SPONSORING/MONITORING AGENCY REPORT NUMBER CSP 96-1032-2

11. SUPPLEMENTARY NOTES

Proceedings are in four sections.

12a. DISTRIBUTION/AVAILABILITY STATEMENT	12b. DISTRIBUTION CODE
Approved for public release; distribution is unlimited.	A

13. ABSTRACT (Maximum 200 words)

The Final Proceedings for International Workshop on Gamma Titanium Aluminide Alloy Technology, 1 May 1996 - 3 May 1996

The Topics covered include: Fundamental research issues for understanding the emerging class of Gamma Titanium Aluminide Alloy Technologies

14. SUBJECT TERMS	15. NUMBER OF PAGES
	16. PRICE CODE N/A

17. SECURITY CLASSIFICATION OF REPORT	18. SECURITY CLASSIFICATION OF THIS PAGE	19. SECURITY CLASSIFICATION OF ABSTRACT	20. LIMITATION OF ABSTRACT
UNCLASSIFIED	UNCLASSIFIED	UNCLASSIFIED	UL

NSN 7540-01-280-5500

Standard Form 298 (Rev. 2-89)
Prescribed by ANSI Std. 239-18
298-102

Microstructural Effects in γ-Titanium Aluminides; XD TiAl Alloys as an Example

L. Christodoulou
Department of Materials
Imperial College
London

Influence of Reinforcement on Microstructure

- Refines the grain size
  - Grain structure uniformity
  - Improved workability
- Modifies kinetics of
  - Recrystallization
  - Grain growth
- TiB_2 does not appear to change intermetallic phase transformations or shift phase boundaries
- Complex precipitation reactions with nitrides, carbides and in matrices containing "active" transition elements

Microstructure Development in XD™TiAl

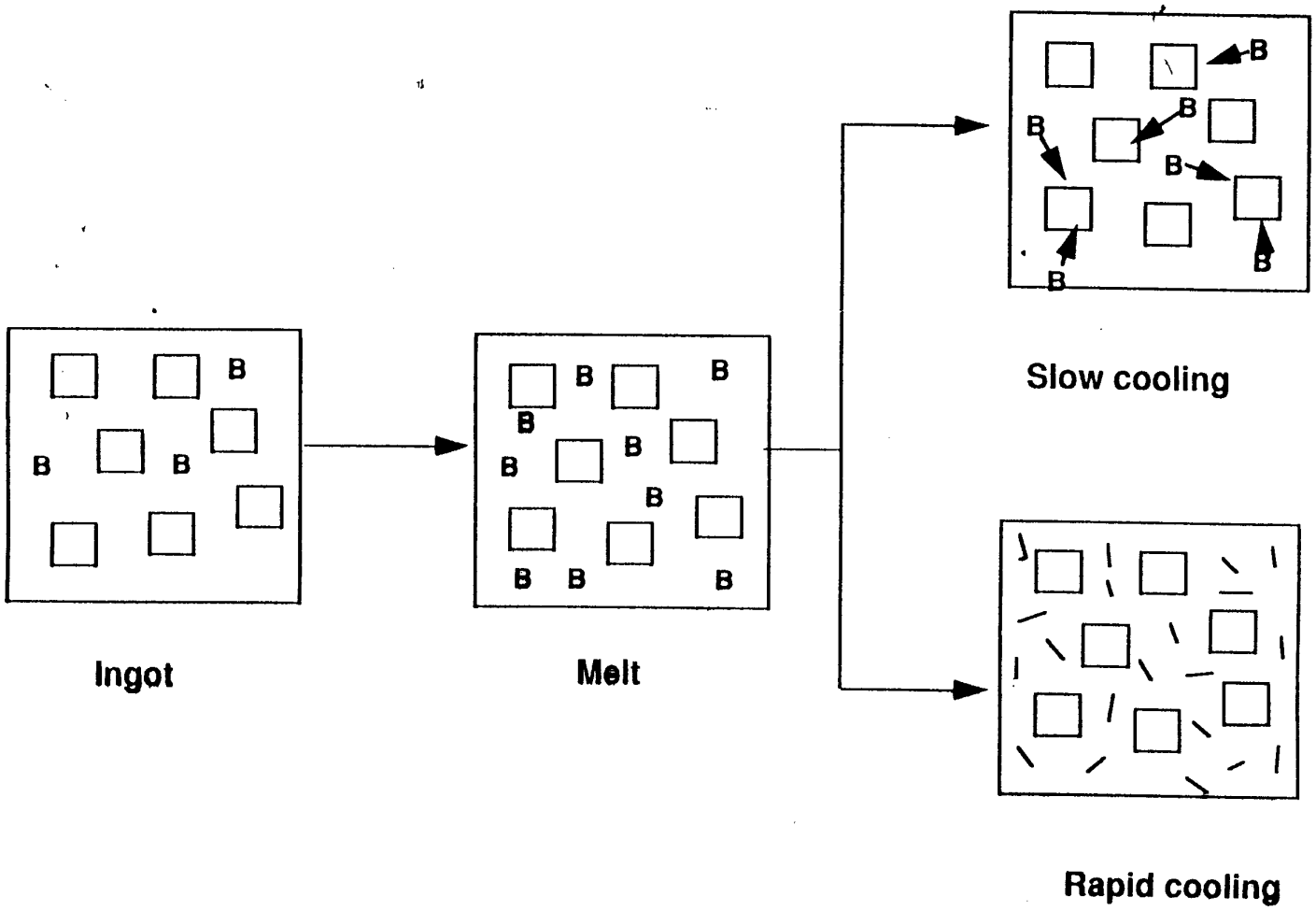

10LC3/31/92

XD™ Processing Applied to TiAl-based Materials

- For gamma-based materials:
  - Investigated tens of reinforcement (borides, nitrides, carbides silicides) /matrix combinations
  - For compositions containing V, Cr, Mn, Fe, Co and Ni TiB_2 is the stable reinforcement
  - For compositions containing Zr, Nb, Mo, Hf, Ta and W the stable reinforcement is (Ti,X)B

XD™ Reinforcement Options

Particulate

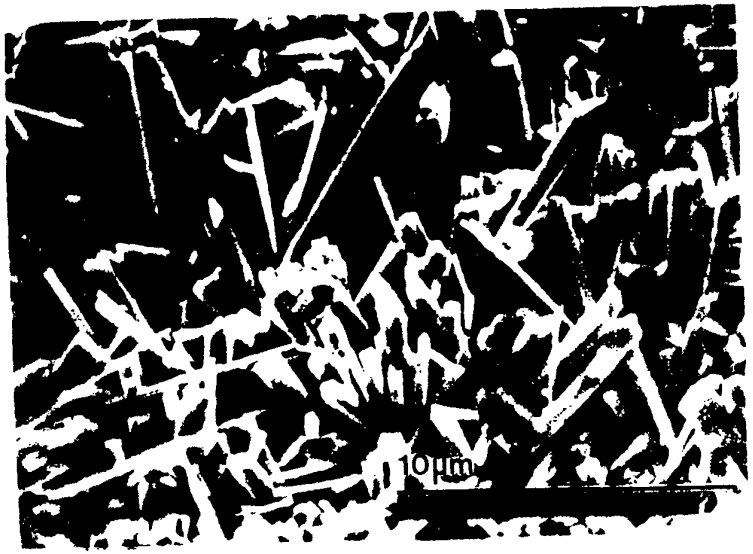

Short Fiber

MARTIN MARIETTA

Grain Size versus Reinforcement Loading

- Grain refinement occurs at low volume fractions of TiB_2, and remains essentially constant to 12 v%.

HONEYWELL CORPORATION

CAST XD™ TITANIUM ALUMINIDE COMPOSITES

SOLIDIFICATION STRUCTURE

WITHOUT XD™ 5X

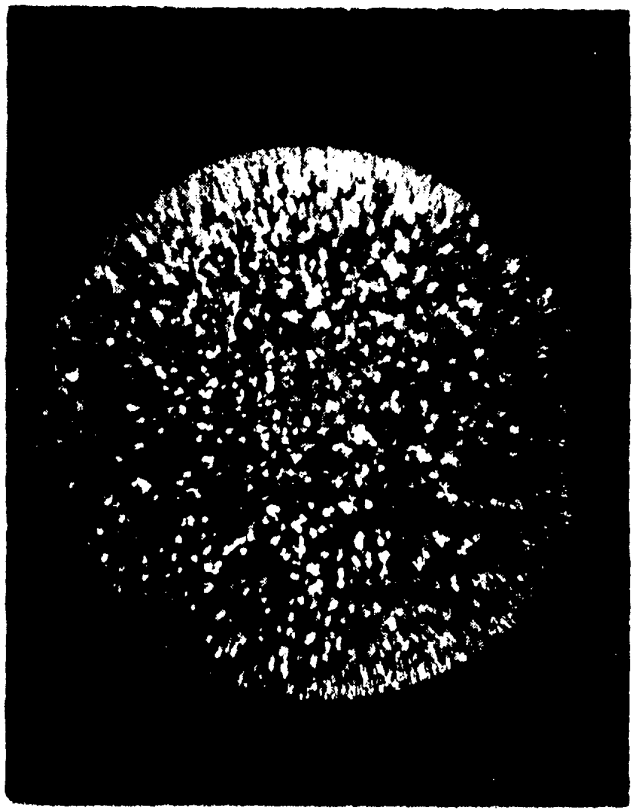

WITH XD™ 5X

- GRAIN REFINEMENT
- INCREASED MICROSTRUCTURAL UNIFORMITY
- STABLE MICROSTRUCTURE
- PARTICLE STRENGTHENING

HOWMET CORPORATION

GO 88/00 7

ISOTHERMAL FORGING OF TITANIUM ALUMINIDES

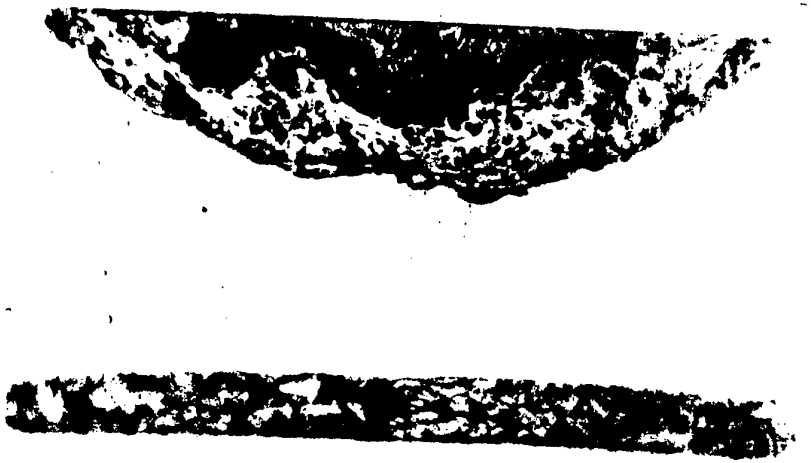

Unreinforced
Ti-45Al

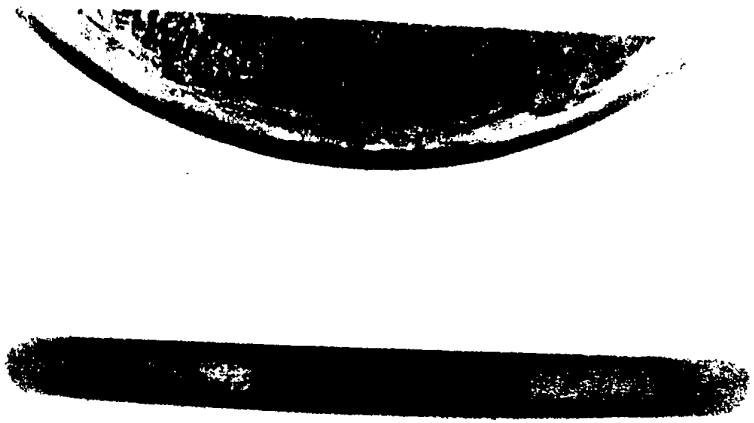

XD™-Reinforced
Ti-45Al-7v/oTiB$_2$

Microstructural Options

Fully Lamellar

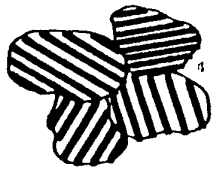

Fully Equiaxed

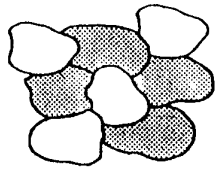

Fully Lamellar (deformed)

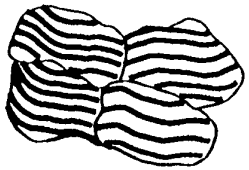

Duplex Structure

Deformed Lamellar / Equiaxed

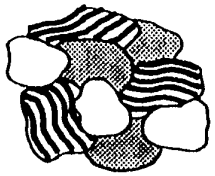

Spheroidized Lamellar

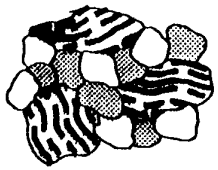

Microstructure Development in XD™ Ti-45Al-7.5 vol.% TiB_2

Extruded

Heat Treated

MARTIN MARIETTA

PHASE MORPHOLOGY OF XD™ Ti-ALUMINIDES: COMPARISON WITH BASE ALLOY

Heat Treated Condition

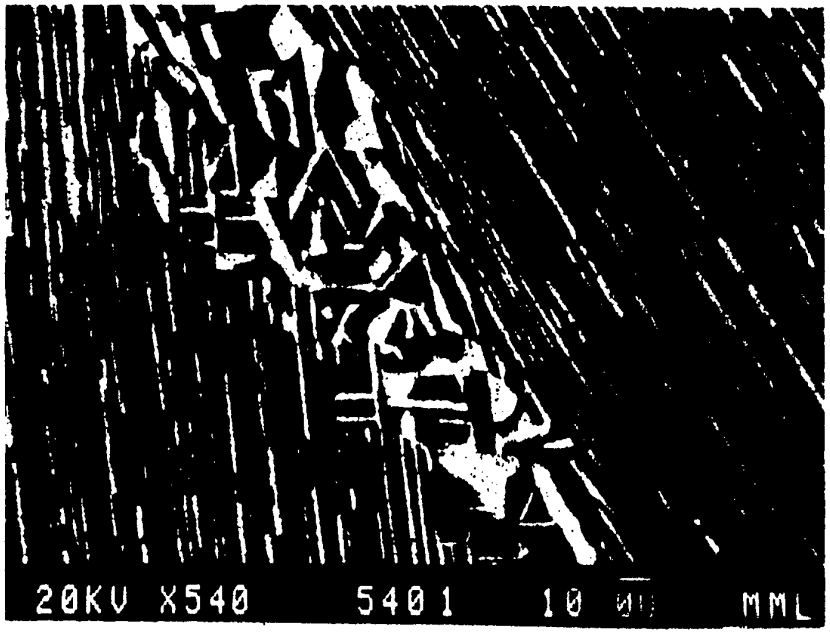

Ti-45 a/o Al (Base Alloy): As-Extruded + 1200°C/16 hr

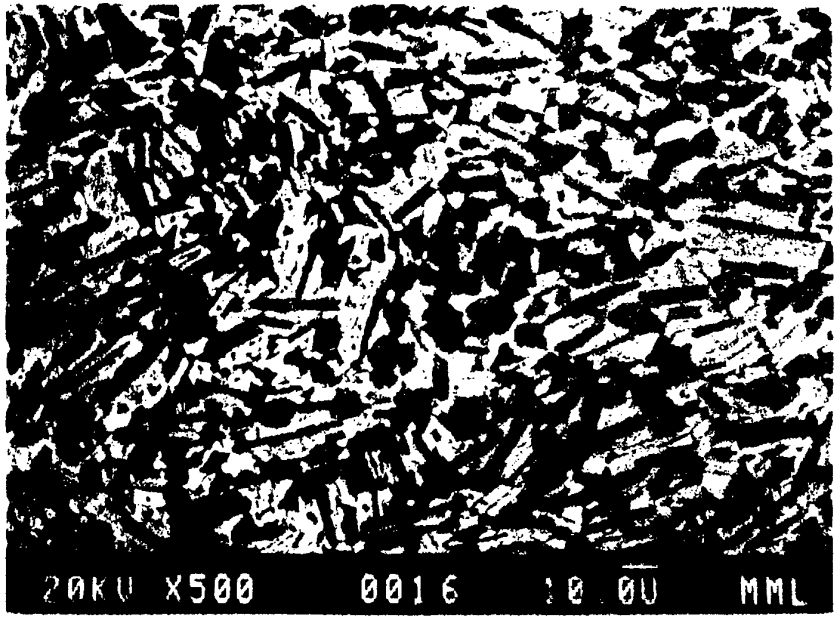

XD™ Ti-45 a/o Al + 7 v/o TiB_2: As-Extruded + 1200°C/16 hr

Ti-46Al: Extruded then Aged 5 Hours at 1200°C

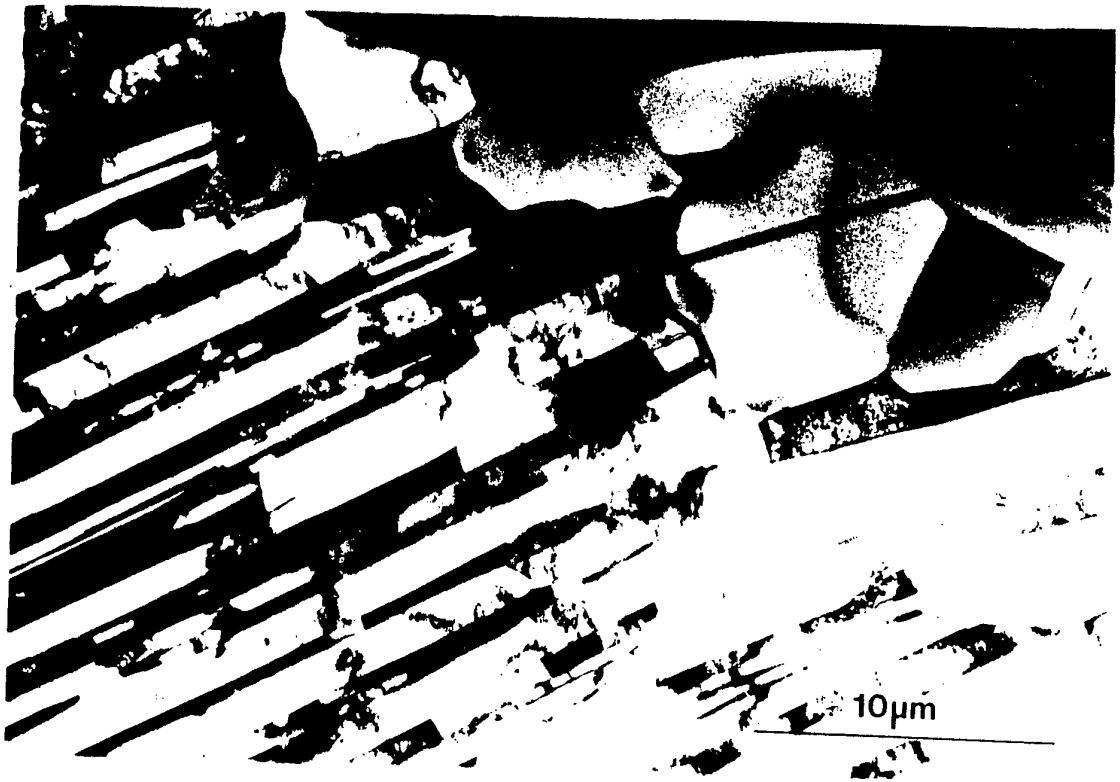

Bright Field Image Taken at $[110]_{\gamma}/[11\bar{2}0]_{\alpha_2}$ Zone Axis of Lamellae

MARTIN MARIETTA

Strengthening Contributions

Direct

Inherent strength of the matrix

Particulate

Indirect

Refinement of microstructure

Mechanical influences of elemental boron in solid solution

$$* \ \sigma_c = \sigma_o + \Delta\sigma_{m,p} + \Delta\sigma_p$$

where σ_c = Strength of the composite

σ_o = Reference stress = strength of base alloy given identical thermal history

$\Delta\sigma_{m,p}$ = Strength increase of matrix due to presence of particulate (indirect effects)

$\Delta\sigma_p$ = Strength increase due to particulate (direct effect)

TiB_2 Reinforcement of XD™ Cast Titanium Aluminides

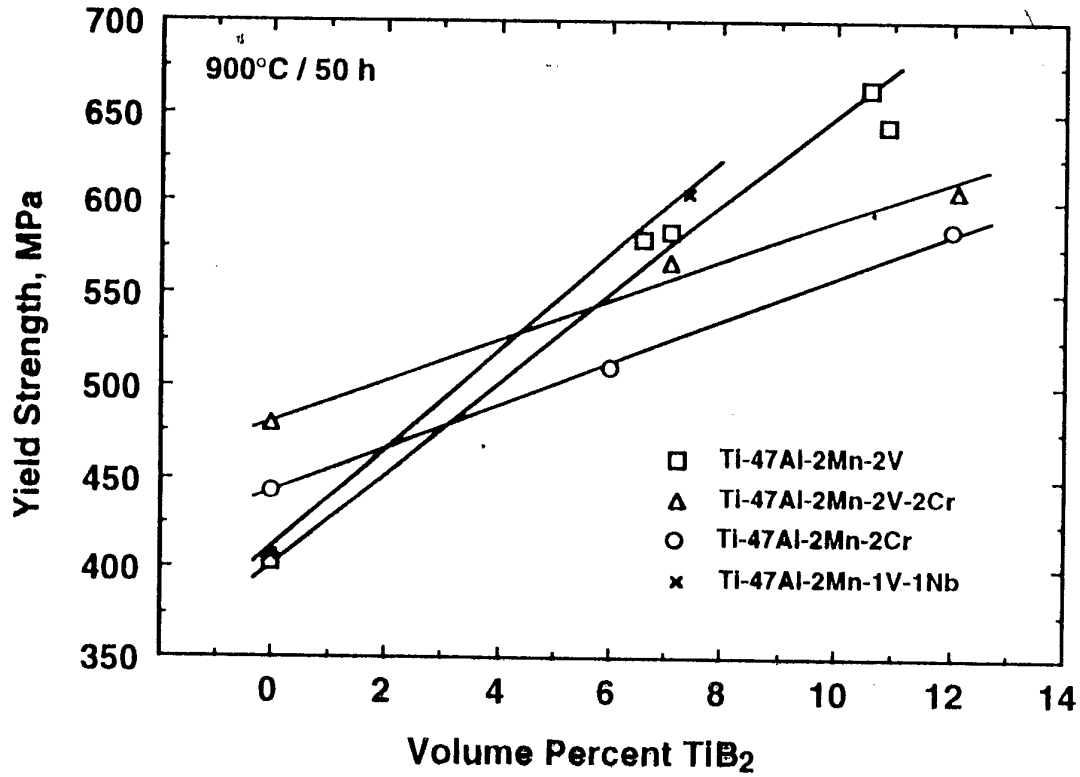

- *Addition of TiB_2 results in strengthening of all titanium aluminide matrices examined*
- *The response to TiB_2 additions varies with base alloy composition*

Direct Strengthening Contributions in XD™ Ti-Aluminides

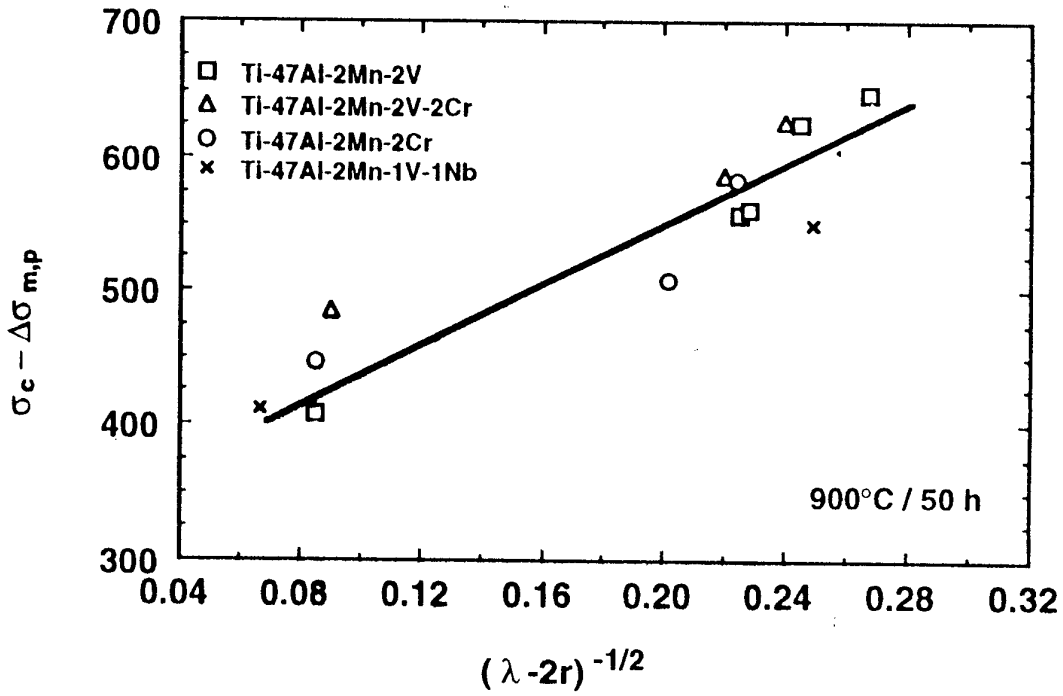

Deformation controlled by strongest "barrier"

Strengthening of XD™ Titanium Aluminide Composites

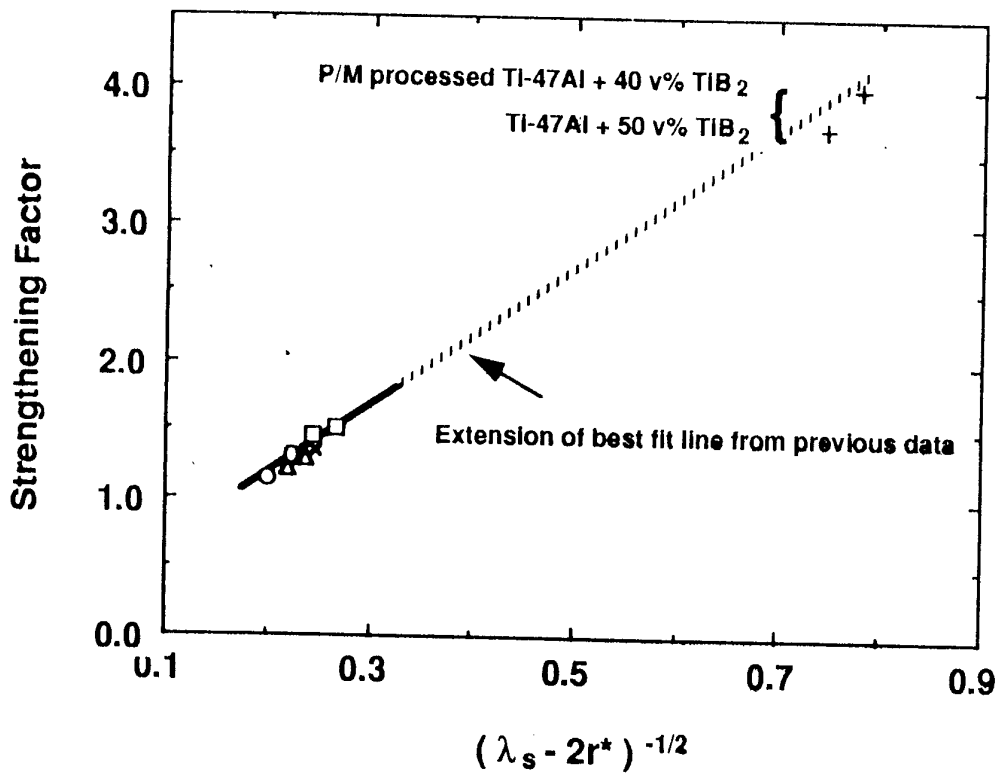

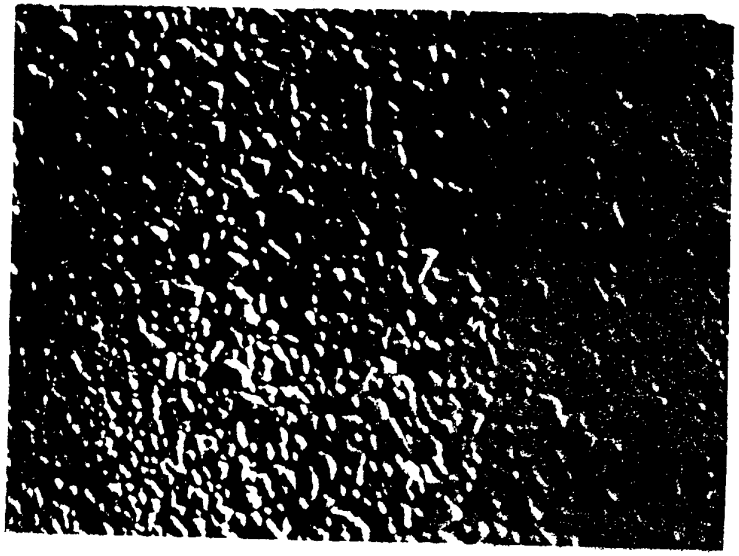

Ti-47Al + 50 v% TiB_2

- ***Correlation of strength to interparticle spacing maintained to high volume fractions of TiB_2 in Ti-47Al***

MARTIN MARIETTA

Plastic Elongation vs Proeutectoid Gamma

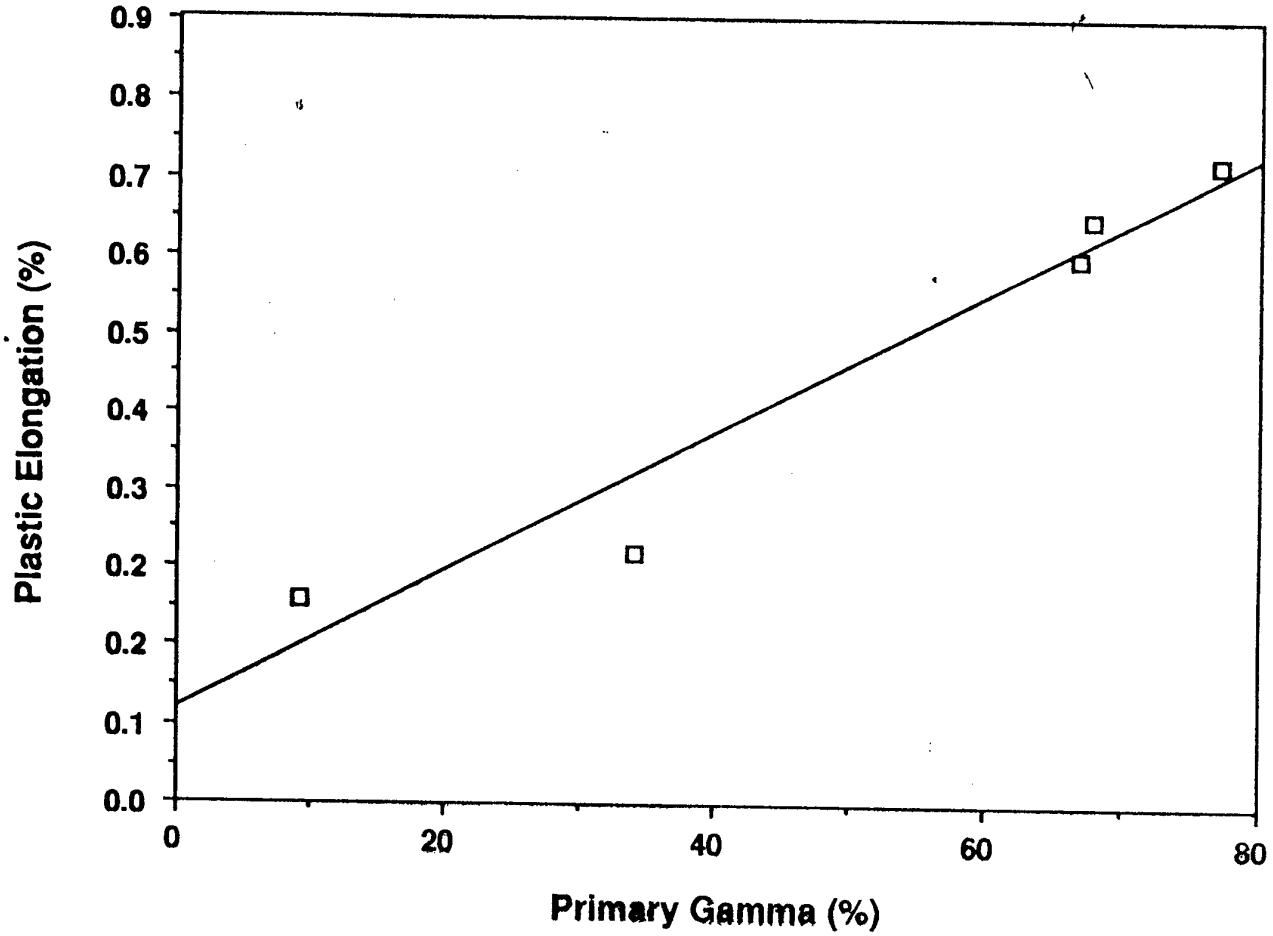

MARTIN MARIETTA

Yield Stress vs Proeutectoid Gamma

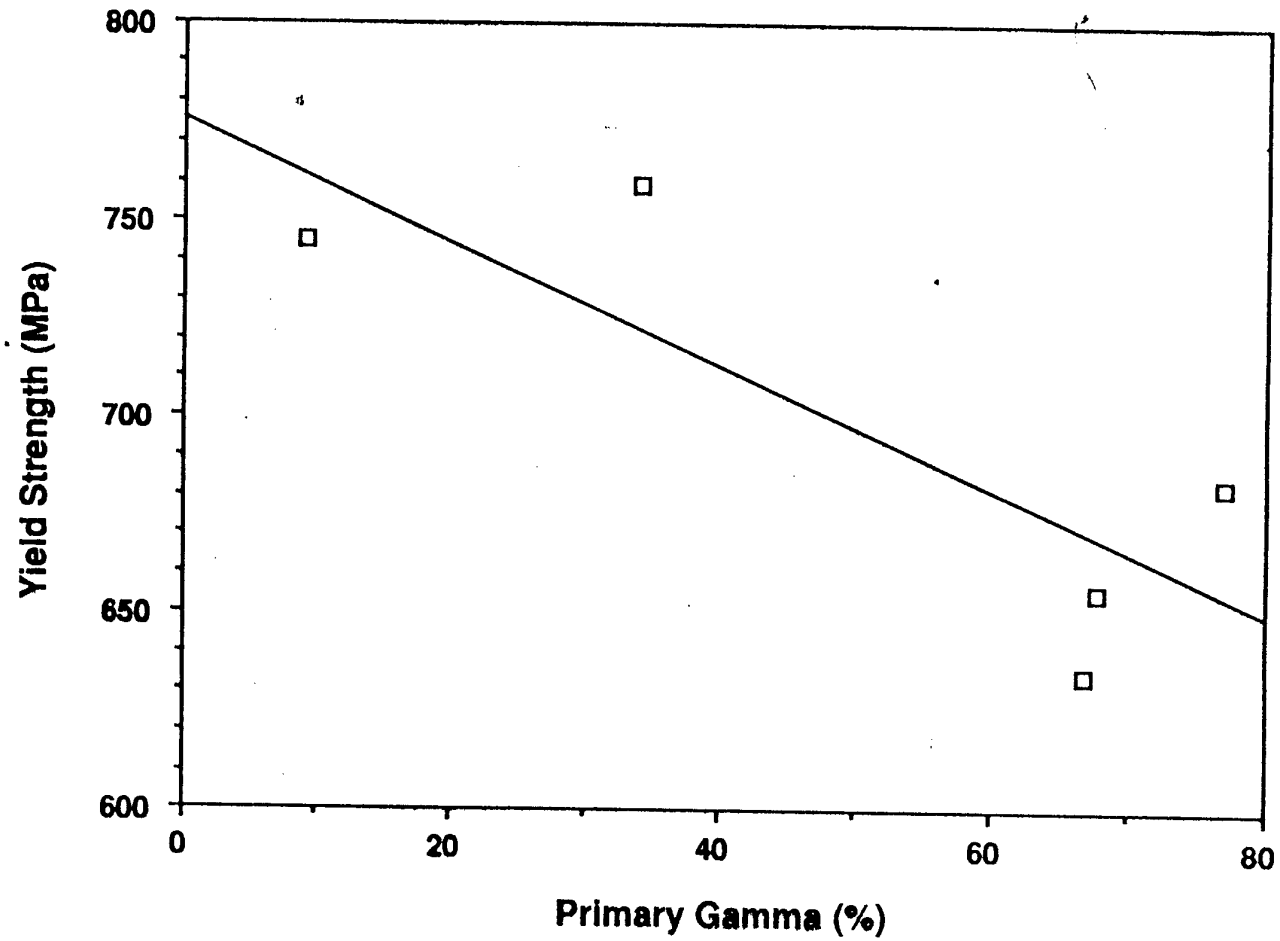

MARTIN MARIETTA

Hardness vs Proeutectoid Gamma

(Vickers Pyramid / 10 kg)

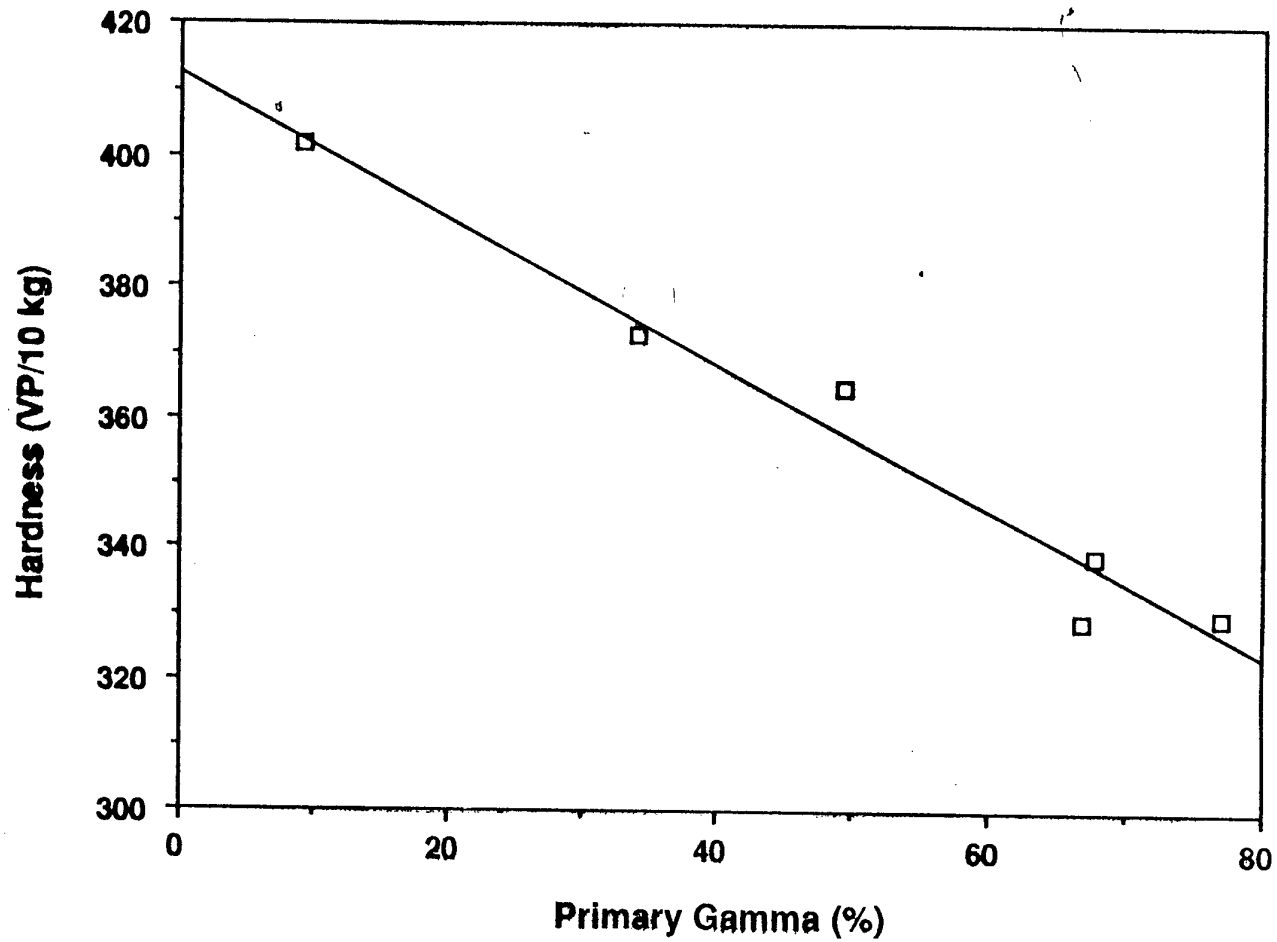

MARTIN MARIETTA

Fracture Toughness as a Function of Microstructure

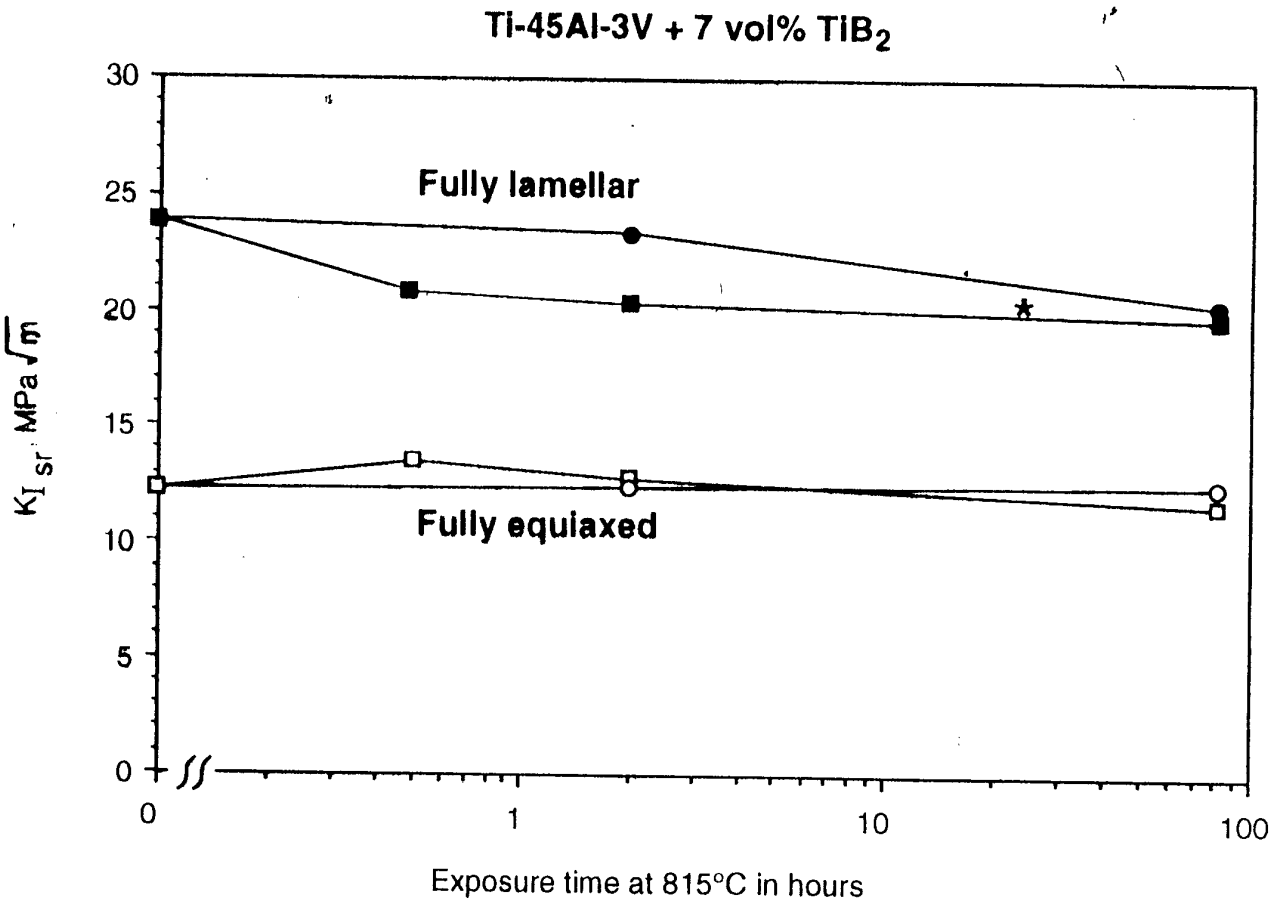

Creep Trends

- Strong grain size dependence
- Lamellar microstructures superior to equiaxed
- Deformed lamellar particularly poor--"dynamic recrystallization" effectively results in very fine grain size and repeated stage I creep
- Reinforcements improve creep (all other microstructural features being equal)

Fracture Toughness as a Function of Microstructure

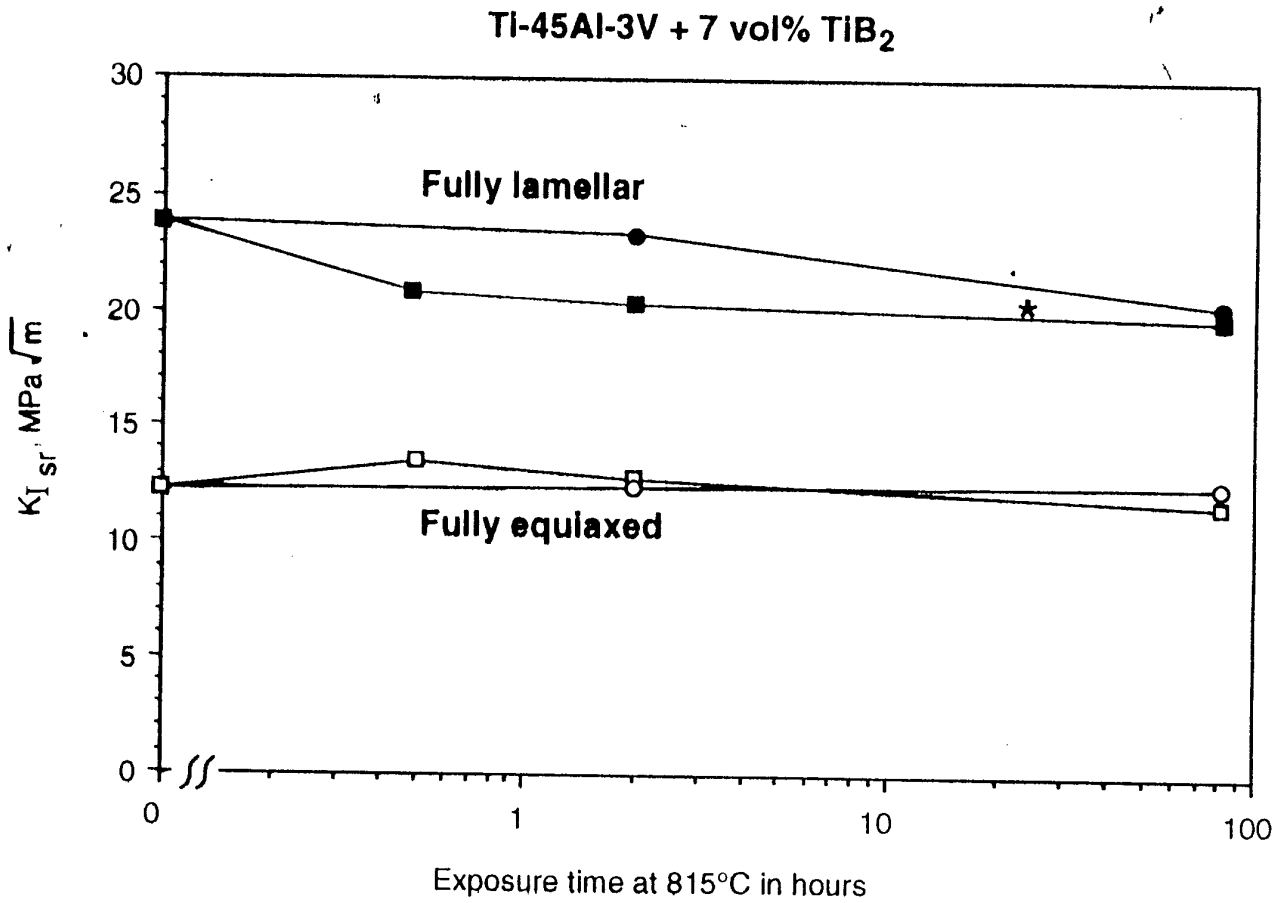

TiB_2 Particle Stability under Service Conditions

Distribution of Particle Sizes by Equivalent Diameter in Ti-43Al-2V + 7 vol% TiB_2

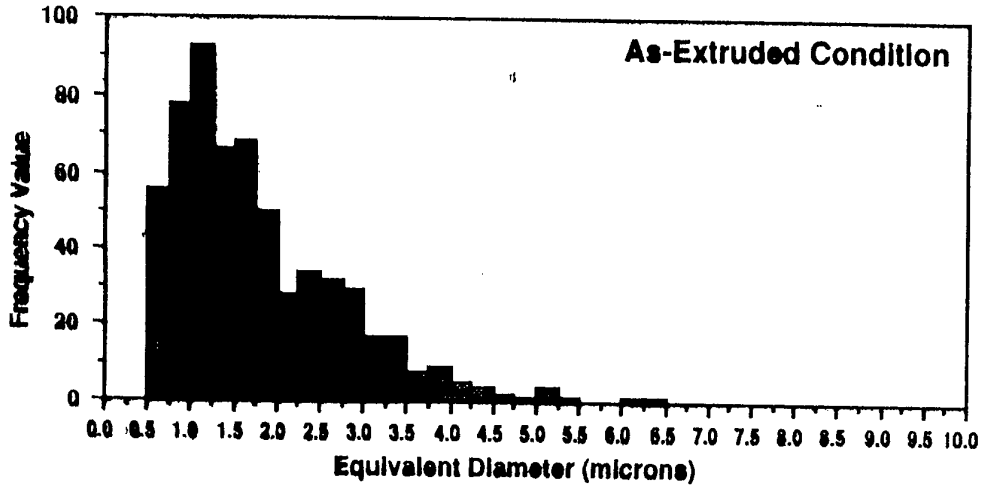

Average Particle
Equivalent Diameter = 1.78 μm
Standard Deviation = 0.98 μm

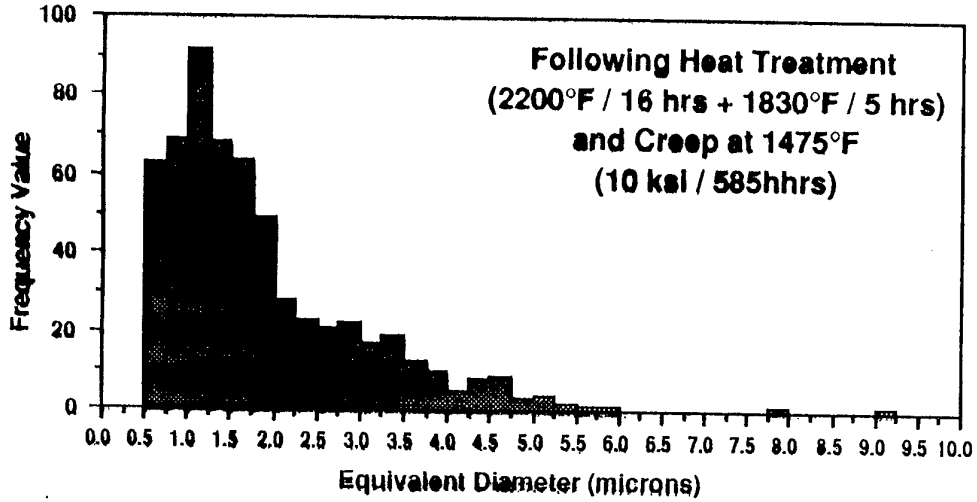

Average Particle
Equivalent Diameter = 1.85 μm
Standard Deviation = 1.15 μm

MARTIN MARIETTA

Grain Size-Dependent Creep Deformation

Ti-47Al

Ti-47Al + 7 v% TiB_2 (Particulate / Equlaxed)

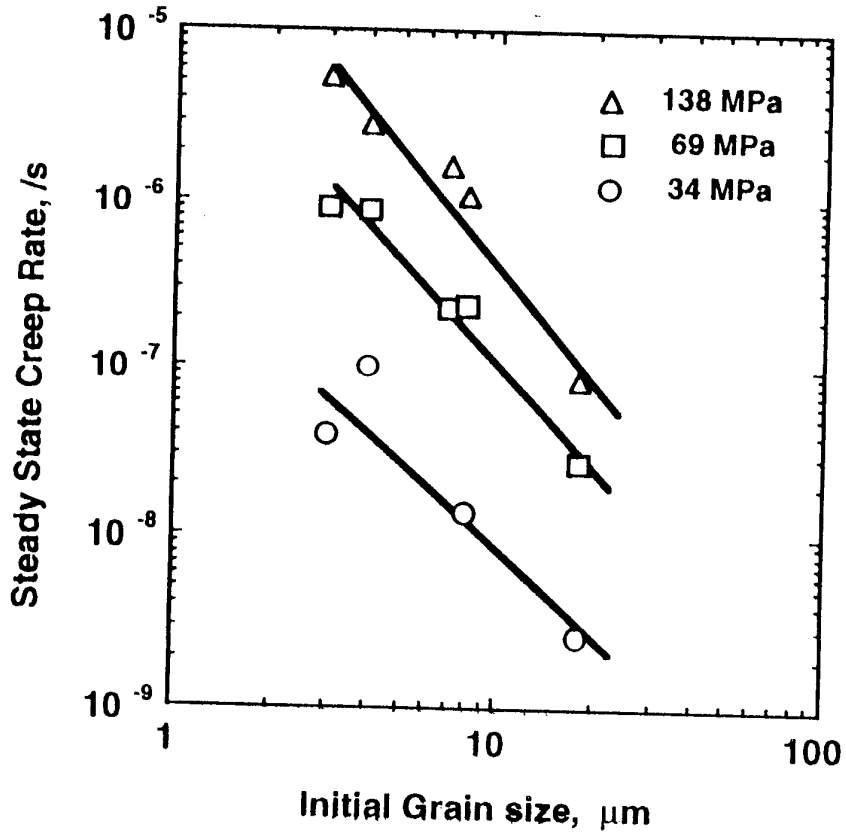

Matrix-Dependent Mechanisms of Creep Deformation

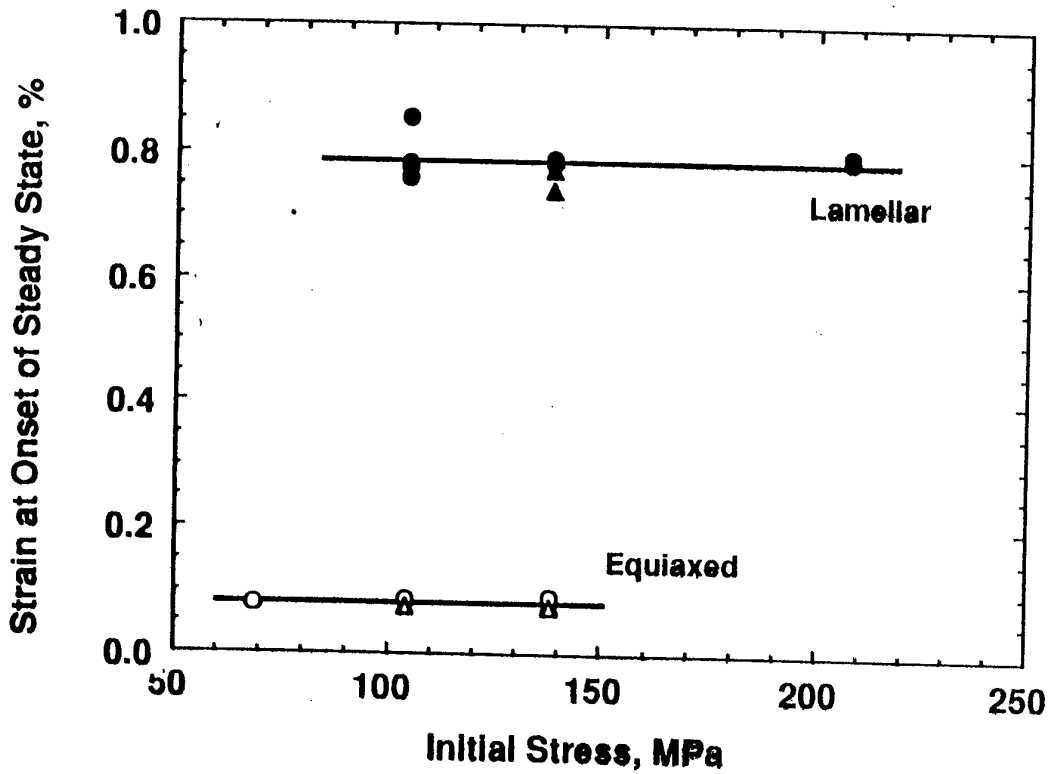

Investment Cast and Forged

Ti-48Al-2V + 7 v% TiB_2 Particulate

Ti-48Al-2Nb + 7 v% $(Ti,Nb)_x B$ Short Fiber

Lamellar

Cast or Forged plus Heat Treatment

Equiaxed

Forged plus 1200°C / 16 h

- Suggests development of a more-extensive dislocation population in lamellar matrices

Creep of XD™ Particulate and Short-Fiber TiAl Composites

Ti-48Al-2V + 7 v% TiB_2 (Particulate)

Ti-48Al-2Nb + 7 v% $(Ti,Nb)_xB$ (Short Fiber)

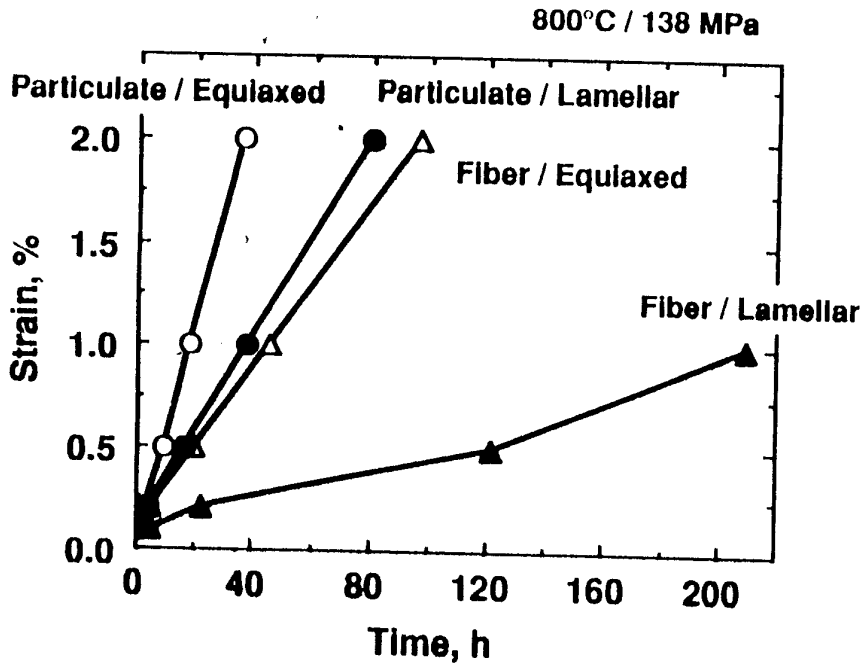

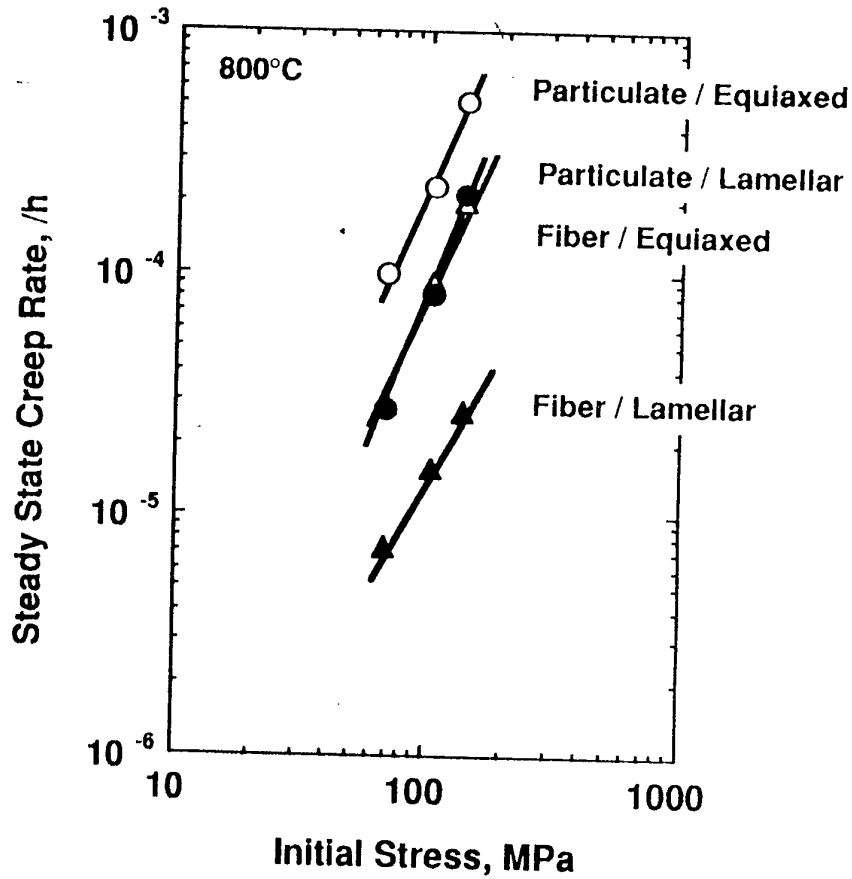

Fiber in lamellar matrix **provides maximum benefit**

MARTIN MARIETTA

Mechanisms of Creep Deformation

$$\dot{\varepsilon}_{ss} = A_o \cdot \exp(-Q_{cr}/RT) \cdot \sigma^n$$

*Equiaxed**		*Lamellar (proposed)*
≈ 3 - 4	Stress Exponent, n	≈ 3 - 4
≈ 300 - 350 kJ	Activation Energy, Q_{cr}	≈ 300 - 350 kJ
$= A_1 \cdot (b/d)^2$	Structure Constant, A	$= f(\lambda^n, \rho, d^p)$?

* For TiAl: Martin et al., 1981;
Kampe et al., 1989;
Takahashi et al., 1991

27LC3/31/92

May 1, 1996

Joint EOARD / IRC International Workshop
on
Gamma Aluminide Alloy Technology

Preliminary results on point defects, atomic mobility and creep in model TiAl compounds

Centre d'Etudes de Chimie Métallurgique (C.N.R.S.)
Address: 15, rue Georges Urbain, 94407 Vitry-sur-Seine Cedex, France
Phone : + 33.1.46 87 35 93
Fax : + 33.1.46 75 04 33
Telex : 265 586 F

Types of properties investigated

- Vacancy properties
  From recovery of irradiation-produced vacancies

- Atomic mobility
  From kinetics of atomic order variations
  atomistic mechanism: controlled by vacancy concentration and vacancy migration

- High temperature deformation (creep)
  Connected with dislocation climb:
  directly controlled by self-diffusion, i.e. atomic mobility

MATERIALS

1) High purity and commercial purity binary alloys,

prepared from high purity or commercial purity Ti and Al

Composition: $Ti_{1-x}Al_x$ with x = 48-50-51.5-53-54.5-56 at%

Processing route

Levitation melting and drop casting + remelting on cooled copper boat and directional solidification

Impurity determination in starting materials:

by activation analysis

Metallic impurities: neutron irradiation

Oxygen: charged particle (^3He ions) irradiation

	Impurity content (wt ppm)	
Metal	Commercial Purity	High Purity
Titanium	Ti 40 (sponge) O = 2500 ± 200 typical: Fe = 100 to 1100 Si = 50 to 100	Ti VA31 (refined by iodide process) O = 27 Fe = 107 Zr = 95
Aluminium	Al6174 (double-electrolysis) Fe = 3.3 Mg = 17 Si = 120 Zn = 8	Al H3GS67 (zone refined) Total ≤ 1

2) Quaternary alloy: $Ti_{48}Al_{48}Nb_2Mn_2$ (CEASI), for creep tests

Processing route: plasma casting + melting on cooled copper boat and directional solidification.

MATERIALS CHARACTERIZATION

Chemical

Bulk concentrations

Determined by Atomic Emission Spectroscopy (ICP - AES)

In high-purity binary TiAl alloys: 50 - 56 at% Al:
bulk concentrations consistent with nominal composition
(deviations < 0.3 at%, usually 0.1 at%)

Homogeneity

Characterized by local X-ray emission (SEM - EDX)

- Al-rich binary TiAl alloys, 50 - 56 at% Al
  (homogenized 24 h at 1125 °C)

  Ti-56 at% Al is homogeneous
  (instrumental standard deviation = 0.25 at%)

  less Al-concentrated alloys: some residual heterogeneity
  (standard deviation of concentration = 0.5 to 1.4 at%)

- Ti-48 at% Al alloys (high purity and commercial purity) and
  $Ti_{48}Al_{48}Nb_2Mn_2$:

  concentration fluctuations (after directional solidification)

in $Ti_{48}Al_{48}Nb_2Mn_2$:

Ti is fairly homogeneous
Al fluctuations of amplitude typically ≈ 2 at%
Nb and Mn: fluctuations anti-correlated to those of Al

MATERIALS CHARACTERIZATION

Structure

Methods:

Optical, SEM, TEM observations, X-Ray diffraction

Results

- Al-rich binary alloys 50-56 at% Al, homogenized 24 h at 1125°C:

  single phase γ, equiaxed grains

  (in the Ti-50at%Al, presence of a very small amount of γ lamellae and α_2 particles)

- Ti-48at% Al (high purity and commercial purity), Ti_{48}-Al_{48}-Nb_2-Mn_2
  (after directional solidification)

  - large grains of lamellar $\gamma + \alpha_2$ structure, elongated in the direction of solidification

1. VACANCY MIGRATION

Experimental

Materials: single-phase γ TiAl

Homogenized high purity alloys
composition: 50 to 54.5 at% Al

Production of point defects

low temperature (21 K) irradiation with 2.5 MeV electrons

Defect elimination

investigated by
residual electrical resistivity measurements,
during isochronal anneals
at increasing temperatures, in range 21 K - 800 K

1. Vacancy migration

Recovery of low-temperature electron-irradiated high-purity single-phase γ TiAl alloys

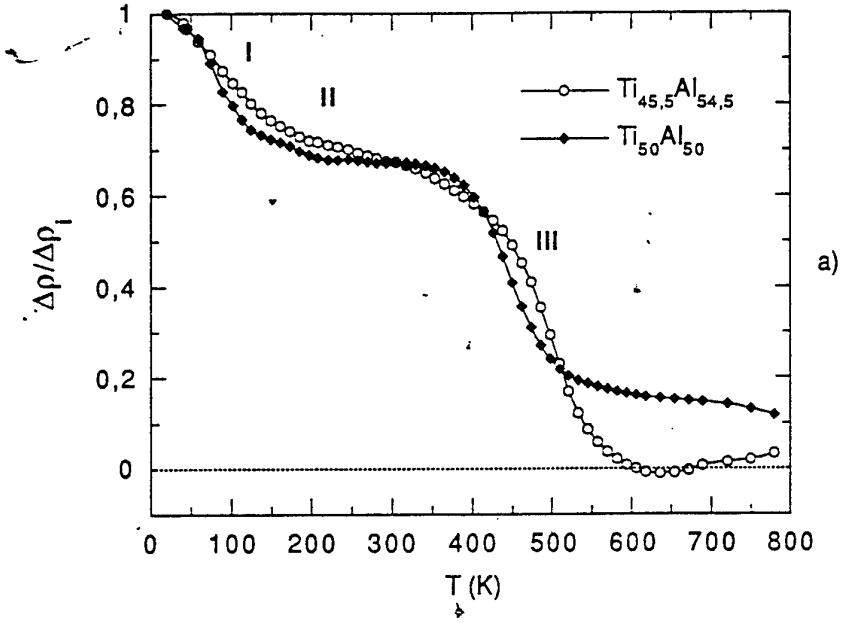

a)

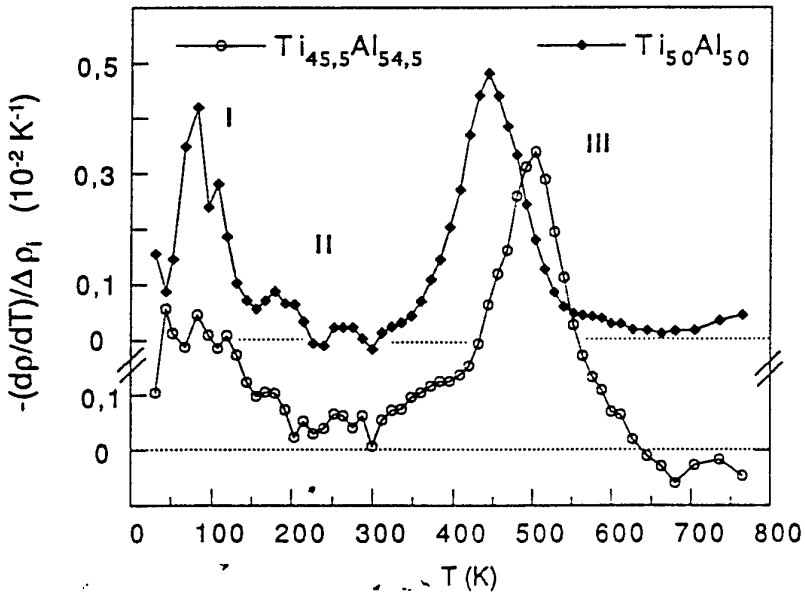

b)

1. Vacancy migration

Results

2 main recovery stages, at ≈ 80 K and at ≈ 440 to 510 K

- Stage I assigned to close-pair recombination and self-interstitial migration
  position nearly independent of alloy composition

- Stage III assigned to vacancy migration (to be confirmed by positron lifetime measurements)
  shifted to higher temperature in alloys with higher Al content

Conclusion

Vacancy mobility **de**creases

when Al concentration **in**creases

2. ATOMIC MOBILITY

Materials: single-phase γ TiAl

Homogenized high purity alloys
composition: 50 to 56 at% Al

Method

Analysis of atomic order changes resulting from heat treatments (monitored by residual electrical resistivity measurements)

Qualitative data:
from isochronal annealing curves

Quantitative determination of characteristic parameters (jump frequencies, activation enthalpies) from kinetics of atomic order relaxation

Typical isochronal curve

Order changes during isochronal thermal treatments in TiAl intermetallic compounds

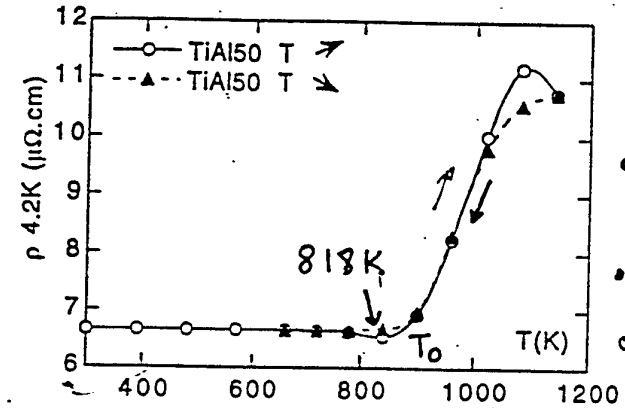

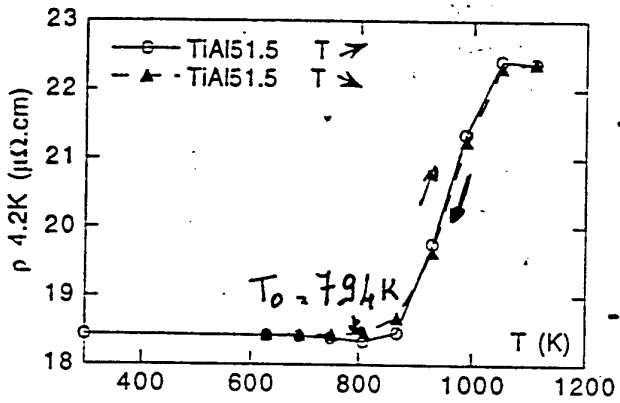

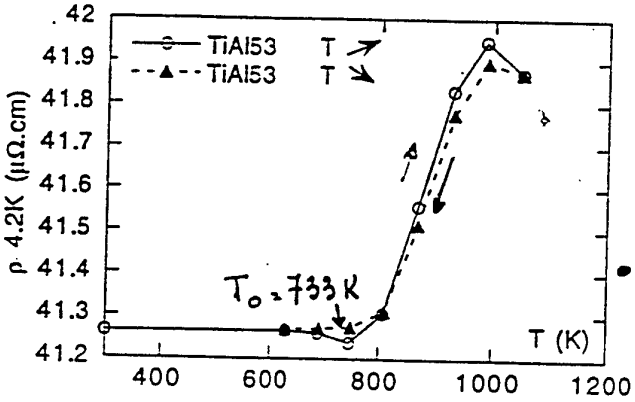

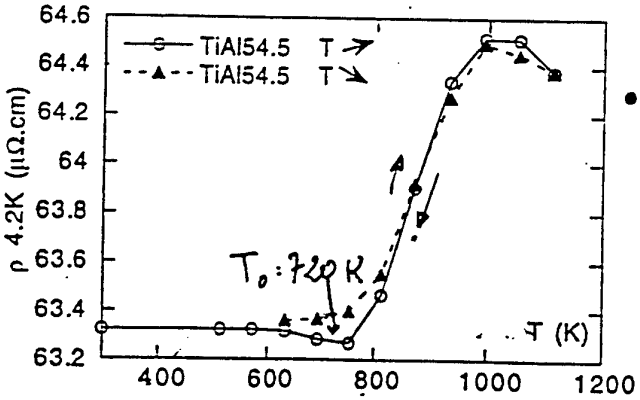

- Same behaviour as in Ni_3Al
- Reversible resistivity variations due to LRO changes
- Composition dependence:
  - amplitude of resistivity variations
  - shift to lower temperatures of atomic mobility onset (T_0) with increasing Al content

⇓

- Atomic mobility becomes faster when deviating from stoichiometry
- At stoichiometry, atomic mobility is smaller than in Ni_3Al (shift by 60K)

COMPOSITION DEPENDENCE OF ATOMIC MOBILITY AND VACANCY PROPERTIES

When **Al** concentration **in**creases,

- Atomic mobility (i.e. atomic jump frequency: ν_{at})
  increases
  (consistent with results of Oikawa et al. (1992)
  creep rate **in**creases with **off**-stoichiometry)

- Vacancy mobility (i.e. vacancy jump frequency: ν_V)
  decreases
- Consequently, vacancy concentration c_V appears
  dependent on TiAl composition. Since
  $\nu_{at} \sim c_V . \nu_V$,
  c_V **in**creases with **in**creasing **Al** content
  (in agreement with vacancy formation enthalpy
  calculations of Badura and Schaefer, 1993)

3. CREEP

Materials: two-phase Ti-48 at% Al alloys

High purity binary Ti-48 at% Al alloy
Commercial purity binary Ti-48 at% Al alloy
Quaternary $Ti_{48}Al_{48}Nb_2Mn_2$ alloy (CEASI)

Processed by melting on water-cooled copper boat and directional solidification

Microstructure in all 3 alloys,
large elongated grains of lamellar $\gamma + \alpha_2$ structure

Creep tests at 800 °C
under high vacuum
compressive stress = 260 MPa

Results

Stationary creep

- in commercial binary and quaternary alloys,

  creep rates are: similar
  (consistent with results of Hayes and McQuay, 1994)

  duration of stationary creep shorter in quaternary than in commercial purity binary alloy

- in high purity binary alloy,
  rate is one order of magnitude larger

Possible mechanism

Impurity (oxygen ?) strengthening of γ phase

Creep tests at 800 °C under high vacuum, compressive stress = 260 MPa

Two-phase Ti-48 at% Al alloys

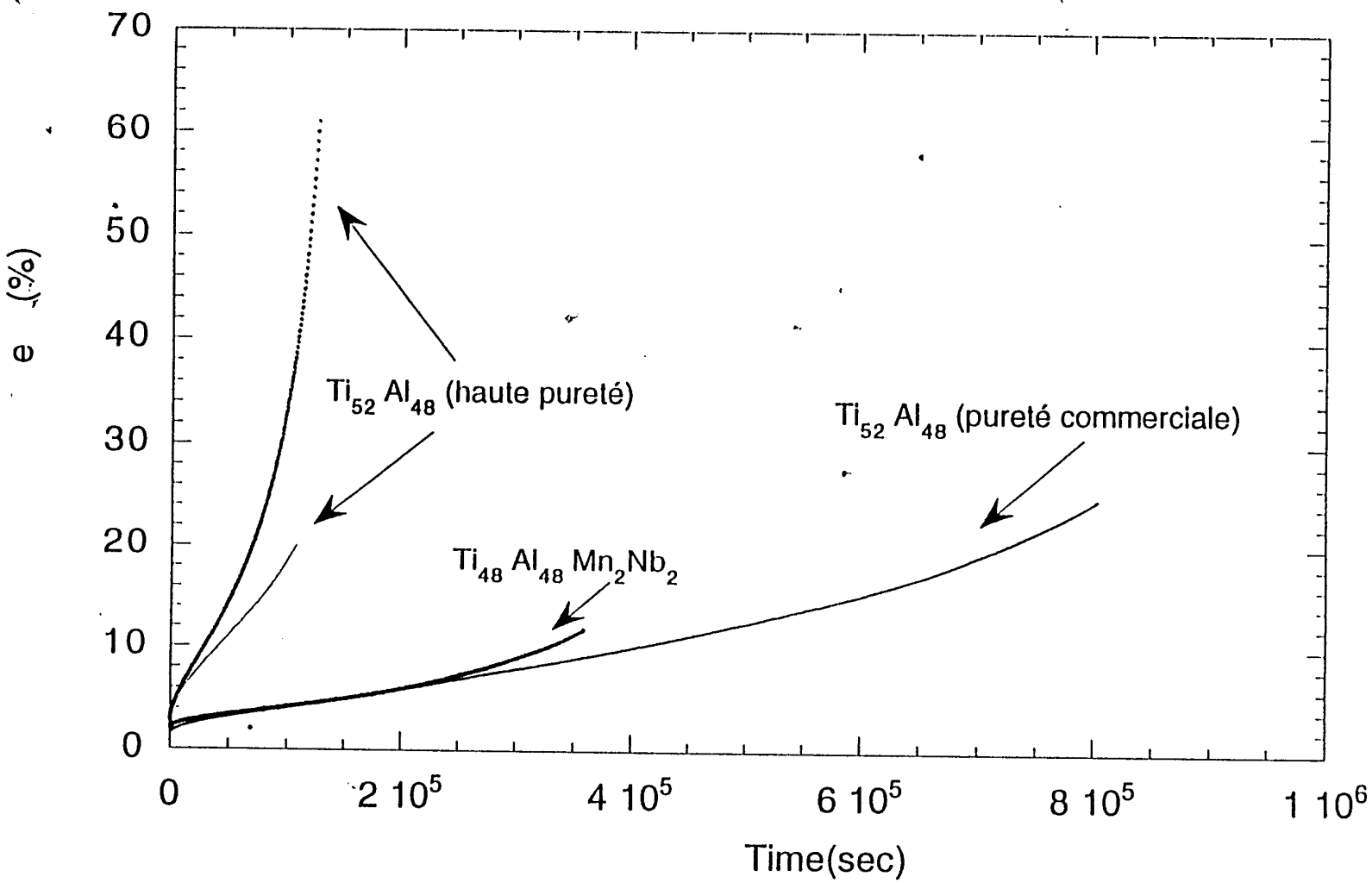

Micro and Macro Segregation Patterns in a PACH Melted Near Gamma Titanium Aluminide

Objectives

To identify the physical and operational parameters which influence solute partitioning and macro-segregation in PACH melted titanium aluminides.

Plasma Melting Furnace: Process Control

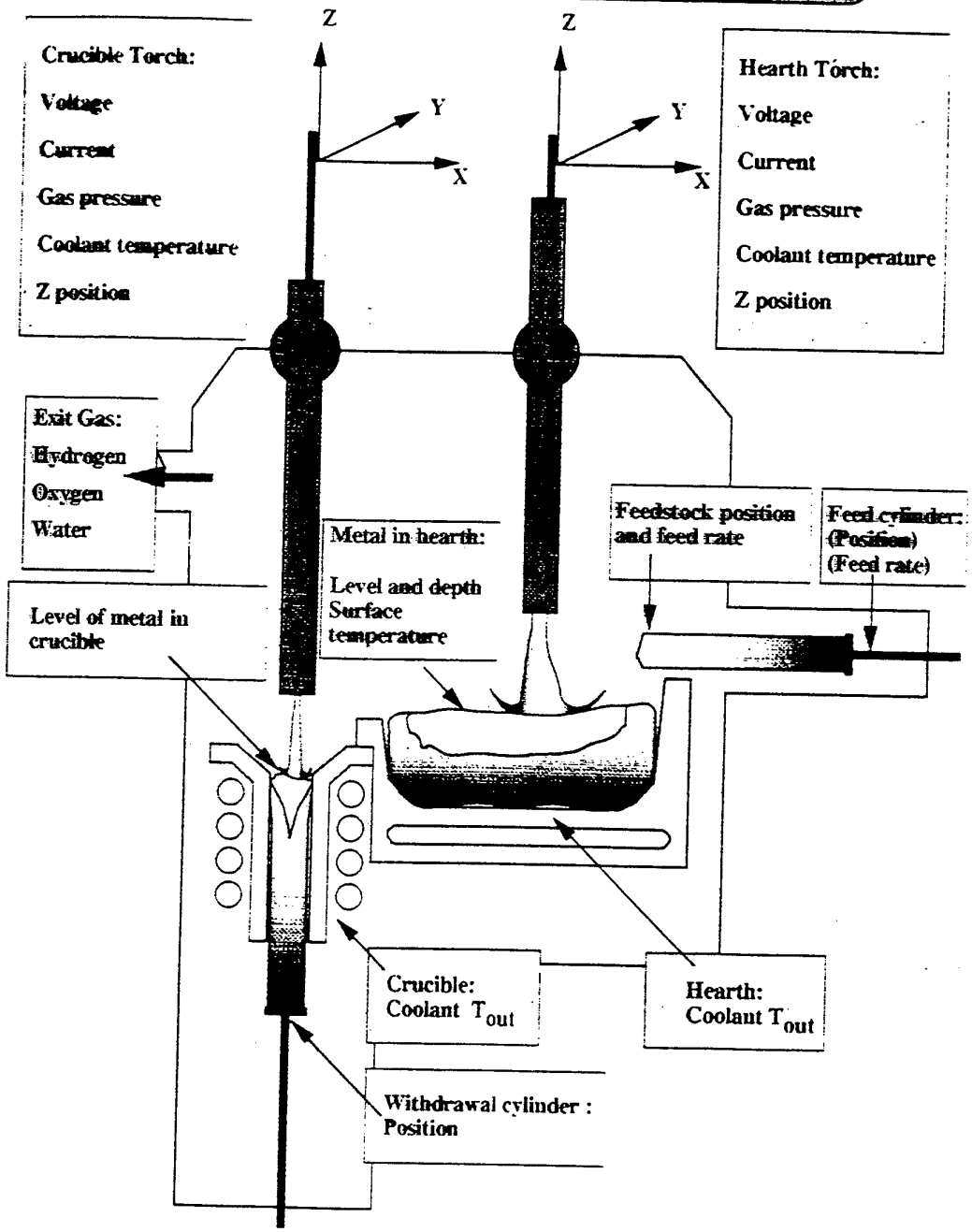

R&D Programme on Evaluation and Minimisation of Compositional Variations in PACH Melted Titanium Aluminides.

- Microstructural and SEM studies to determine the extent of variation in local solidification conditions and to ascertain the levels of micro-segregation.

- Development of quantitative chemical analysis procedures (GD-OES) for assessing the levels and the spatial variations in alloy composition across the ingot.

- Macrostructural and analytical studies to determine the correlations between process parameters, macrostructural development and macro-segregation.

- The development of process monitoring and control procedures to minimise periodic and / or random variations in melting and casting conditions.

Microstructural and SEM Studies

Objectives:

To determine the effects of process conditions on local solidification time and the extent of micro-segregation.

Experimental:

- Grain orientation measurements to determine the depth and shape of the melt pool and its variation with casting conditions.
- SDAS measurements to determine the extent of variation in local solidification time.
- Vertical float zoning to simulate the effects of different solidification rates on SDAS and solute partitioning.
- EDX studies to determine the effects of different solidification and casting conditions on micro-segregation.

Macro / Microstructures Observed in PACH Melted Ti-48Al-2Mn-2Nb

Equiaxed Chill Zone (Edge)

Columnar (Mid-Radius)

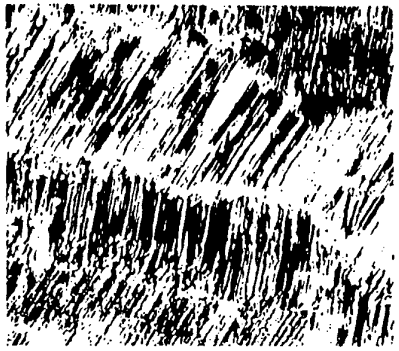

Cored-Columnar (Mid-Radius / Centre)

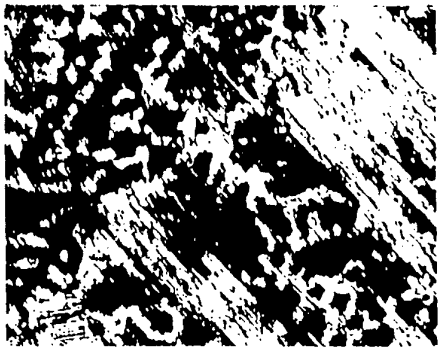

Longitudinal Macro

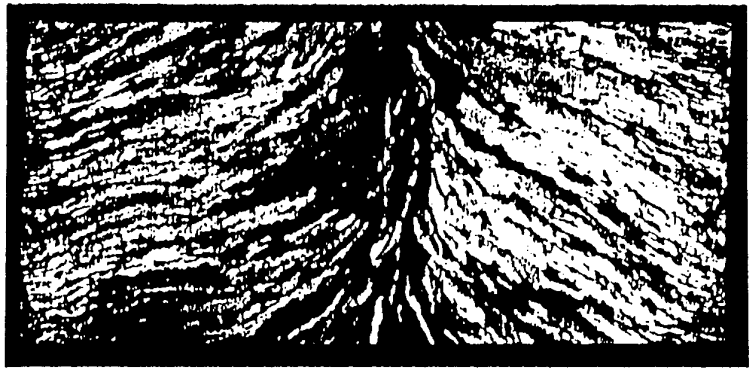

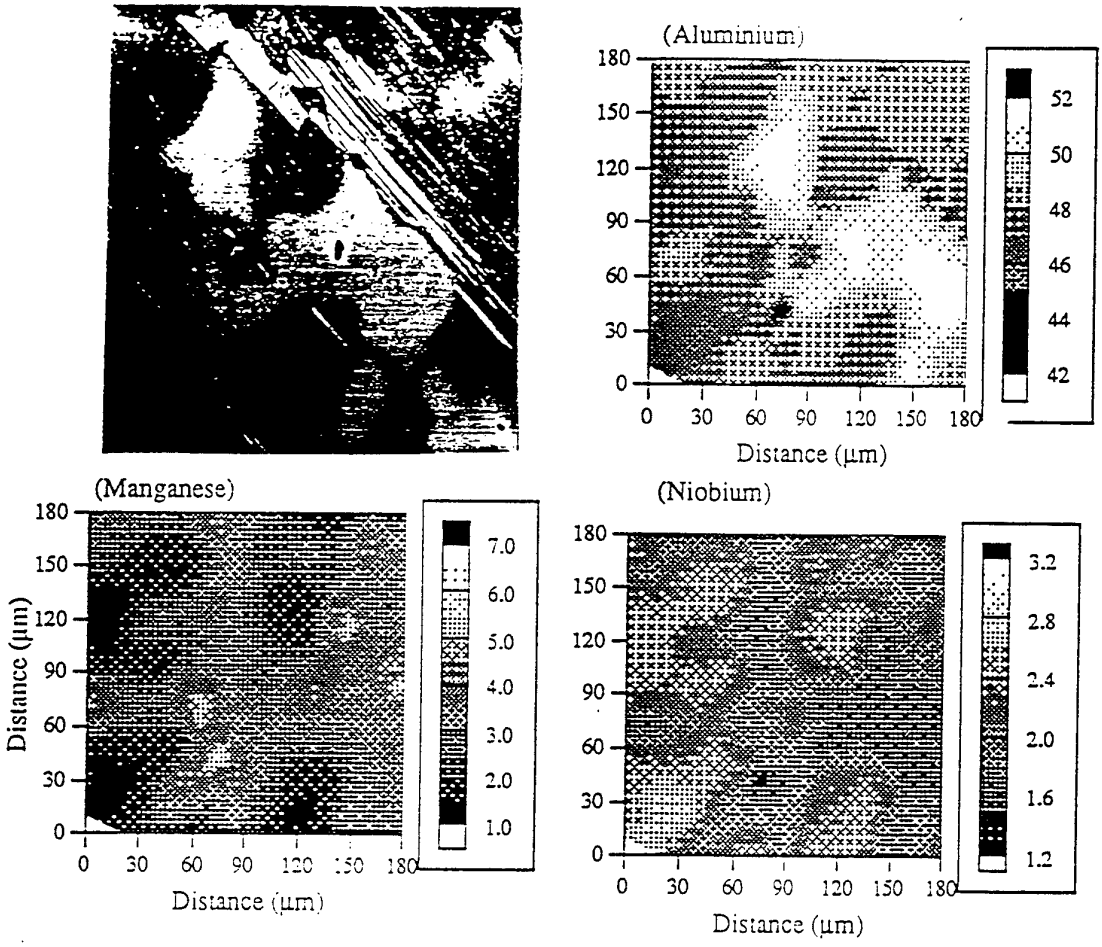

Optical micrograph and EDX analysis plots showing the spatial variations in Al, Mn and Nb within the columnar / dendritic region of PACH melted Ti-48Al-2Mn-2Nb.

SEM Back Scattered Electron Images Showing Dendrite Growth Morphology Within the Columnar Zone

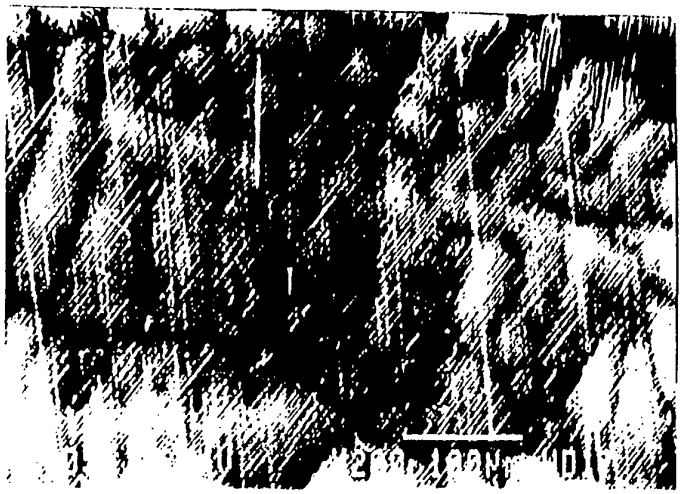

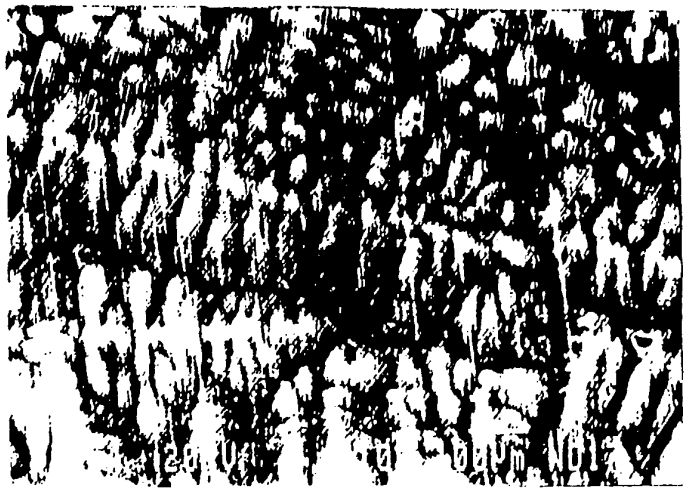

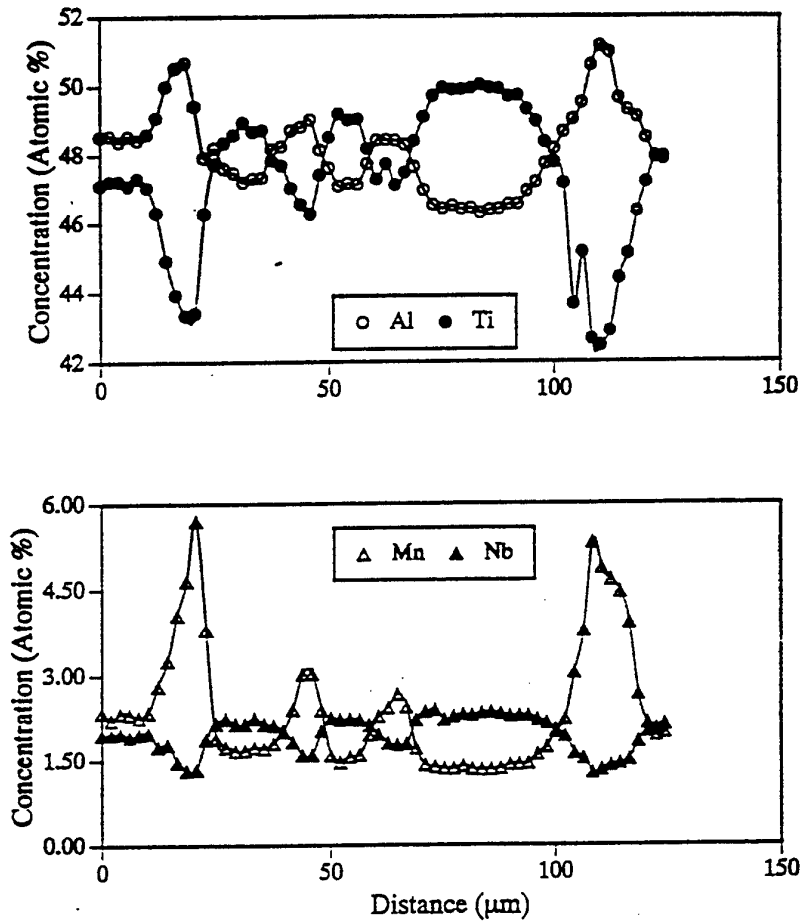

EDX profiles showing compositional variations across the secondary dendrite arms of a hexagonal dendrite observed in float zone melted Ti-48Al-2Mn-2Nb (sample number B1 / Zoning Rate ≈ 0.08 mm/s).

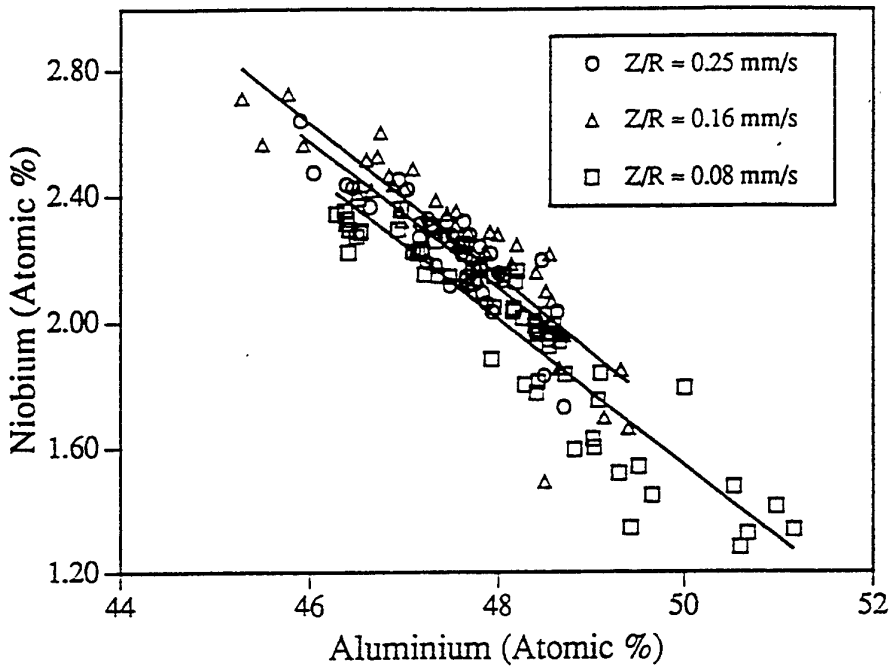

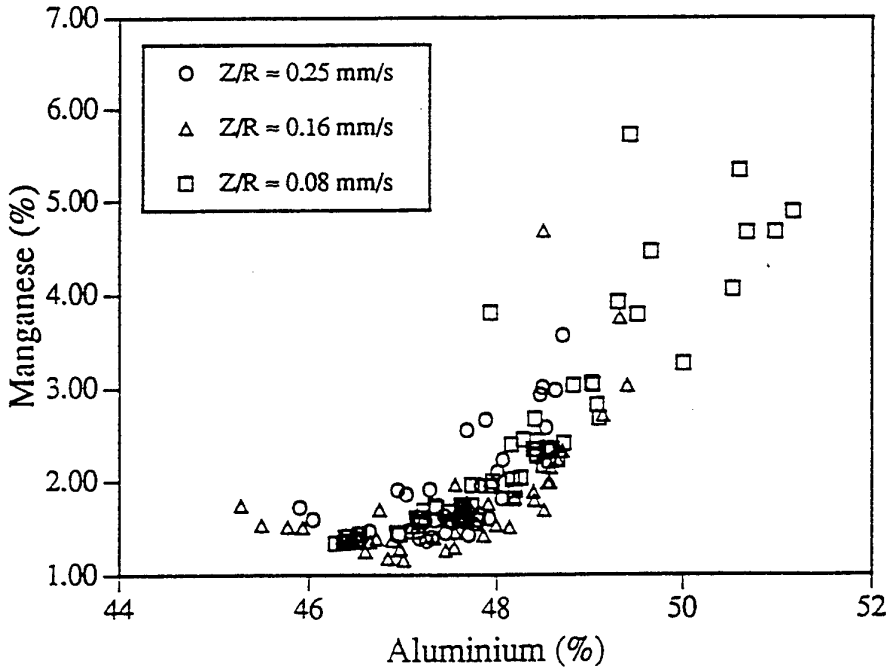

EDX data showing correlations between Al, Nb and Mn segregation in float zoned Ti-48Al-2Mn-2Nb alloy.

EDX Data Obtained from Ingot and Float Zone Melted Ti-48Al-2Mn-2Nb Showing Variations in Al Concentration and Extent of Inter-Dendritic Segregation.

Bar N°	Zoning Rate (mm/min)	Mean	Max	Min	Range	Std Dev	Partition Coefficient (C/C_o)
11	N/A	48.45	50.52	45.17	5.36	1.09	0.94 - 1.05
N/A	4.8	48.14	51.16	46.29	4.88	1.24	0.96 - 1.06
N/A	9.6	47.57	49.41	45.28	4.13	1.03	0.94 - 1.03
N/A	15.0	47.55	48.71	45.90	2.81	0.66	0.96 - 1.01

Glow Discharge Optical Emission Spectrometry

Problems:

Assumes that the intensity of an element x of concentration C_x is linearly dependent on the emission yield k_x and the sputter rate q. Problems arise in that the sputter rate is matrix dependent and the emission yield is dependent on all three lamp parameters (voltage, current and argon flow rate). These parameters are not separately variable.

Experimental:

- Production of chemically homogeneous samples with varying alloy contents for the determination of calibration curves.
- Operational studies to determine voltage, current, flow rate correlation's and the effects on emission yield.
- Determination of sputter rate variations as a function of operating conditions and matrix composition.
- Determination of optimum operating conditions and calibration procedures.

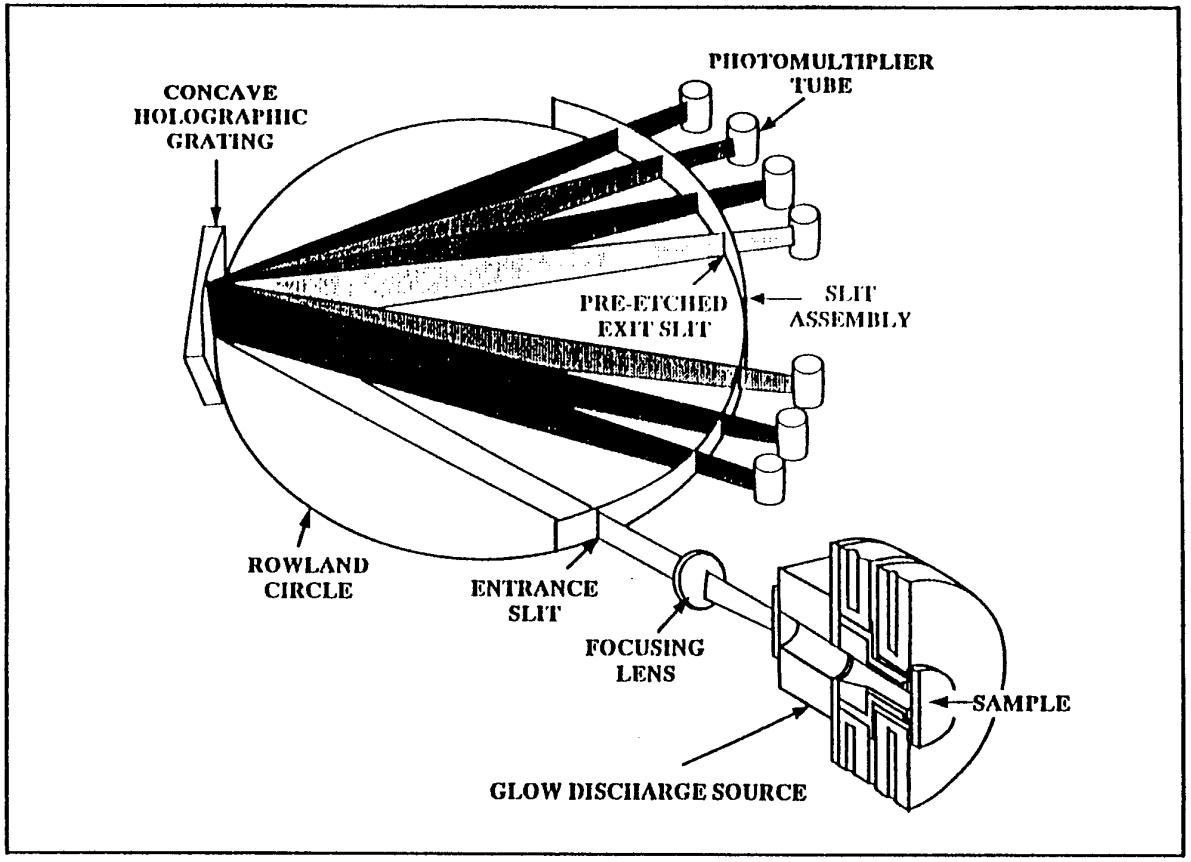

Schematic illustration showing the layout and principal operating features of the LECO GDS Spectrumat 750 Glow Discharge Optical Emission Spectrometer.

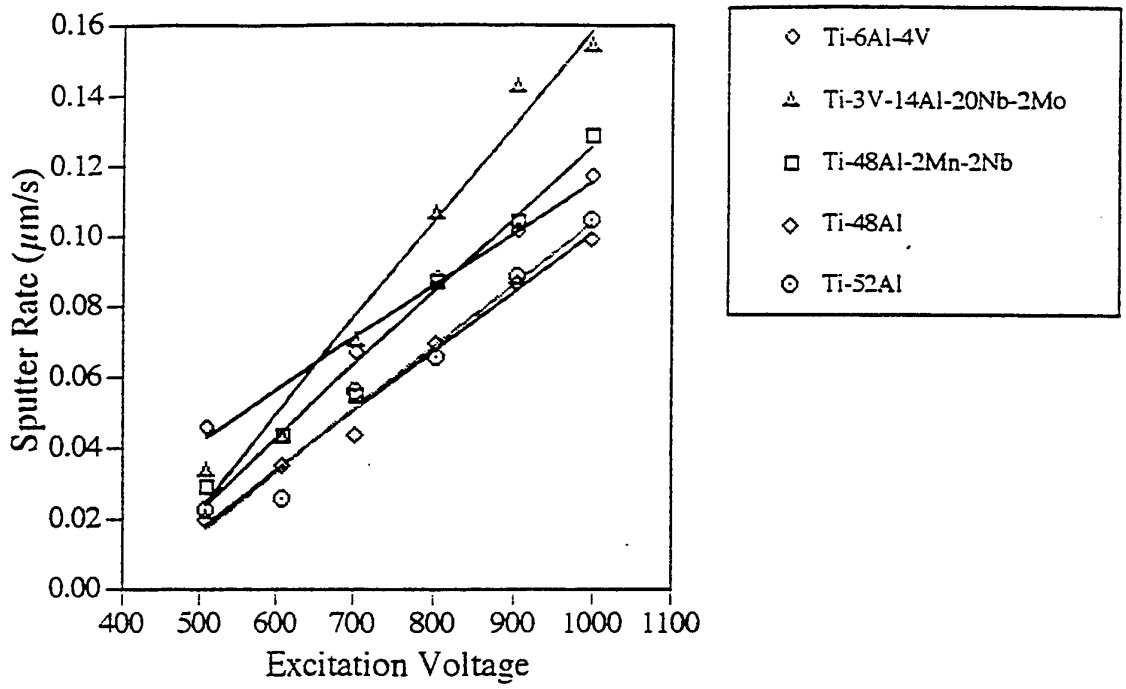

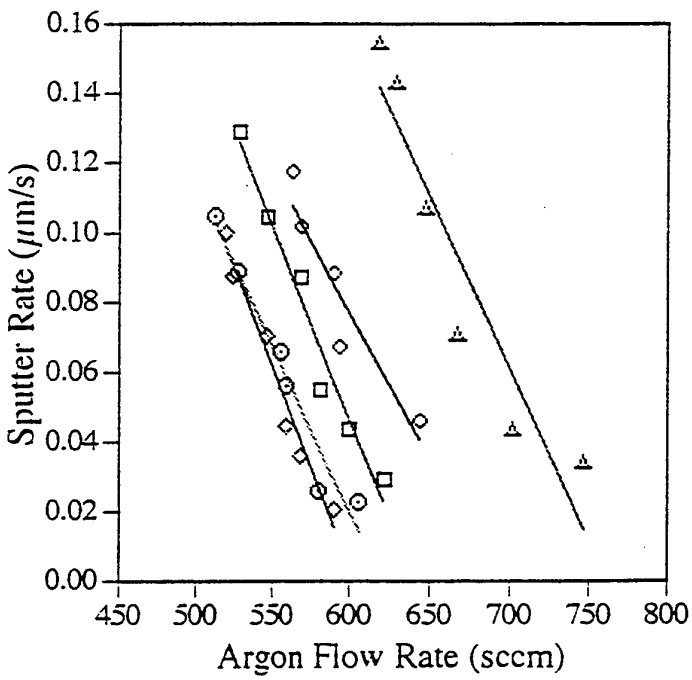

Crater depth measurement data showing possible correlations between sputter rate. excitation voltage and argon flow rate for Ti-Al based

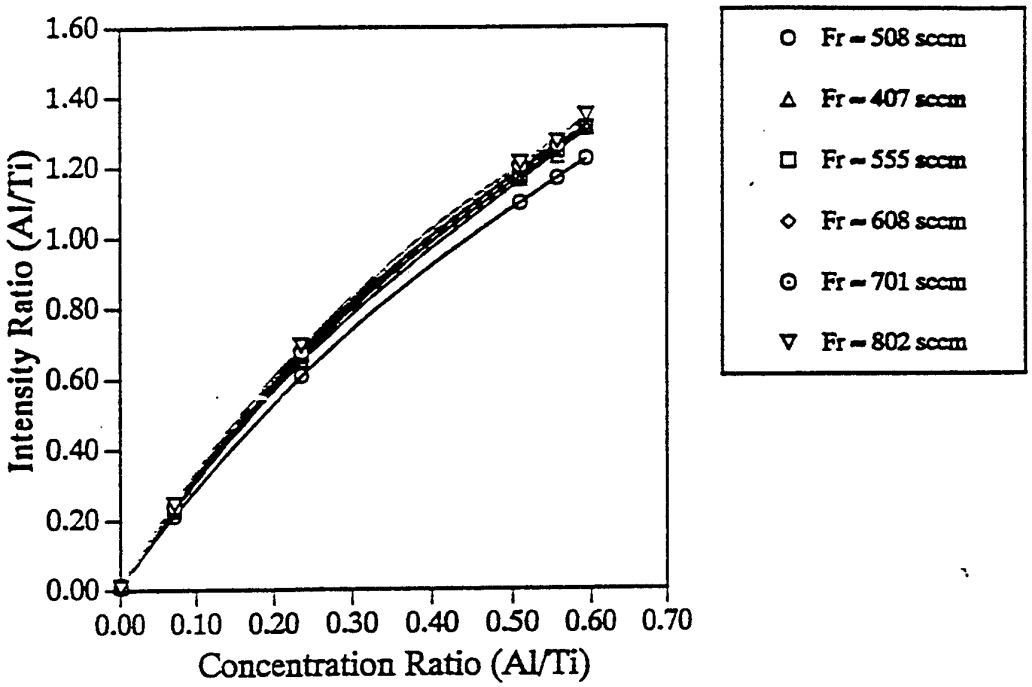

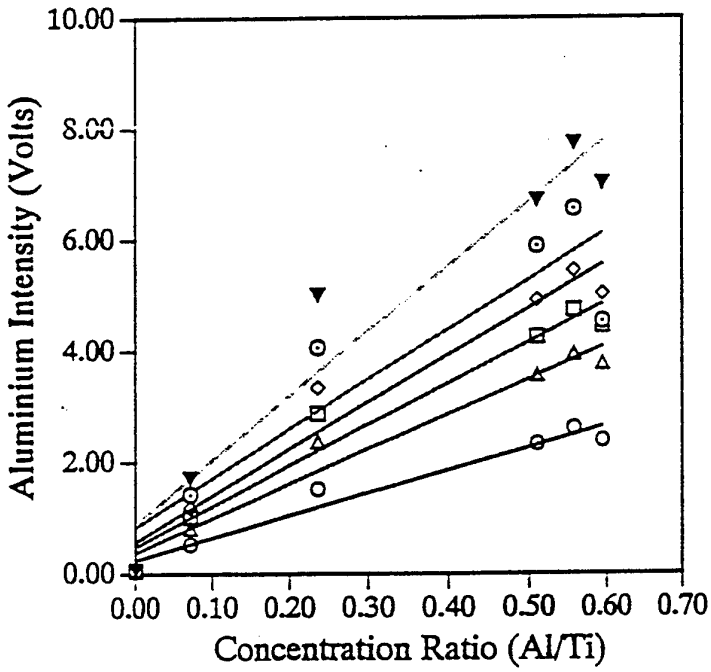

GD-OES calibration curves for Aluminium in Titanium and Titanium / Aluminium alloys showing the effects of variations in Argon flow rate. Excitation voltage and lamp current were controlled so as to maintain a constant applied power of approximately 40 watts.

XRF analysis results showing showing compositional variability in transverse sections taken from Bar N° 11

Slice N°	Al (Wt %)	Mn (Wt %)	Nb (Wt %)	Al (At %)
1	32.7	2.86	4.99	47.36
2	34.10	2.83	4.78	48.92
3	33.50	2.80	4.91	48.26
4	32.70	2.90	5.14	47.40
5	33.40	3.01	5.06	48.18

Comparison of XRF and GD-OES Analysis Results for Bar N° 11

Method	Mean	Maximum	Minimum	Range
XRF	48.02	48.92	47.36	1.56
GD-OES	47.70	50.68	46.42	4.26

Macrostructural and Analytical Studies

Objectives:

To determine the effects process parameters, and in particular the role of transient variations in melting and casting conditions, on macrostructural development and macro-segregation in PACH melted Titanium Aluminide.

Operational Parameters:

- The frequency and rate of transfer of liquid metal between the hearth and the crucible.
- The height, trajectory and power of the crucible and hearth torches.
- The rate of delivery of the feedstock to the hearth.
- The rate of ingot withdrawal from the crucible and the extent of mould oscillation.
- The ingot top position and the level of liquid metal within the crucible.
- The extent of electro-magnetic stirring.

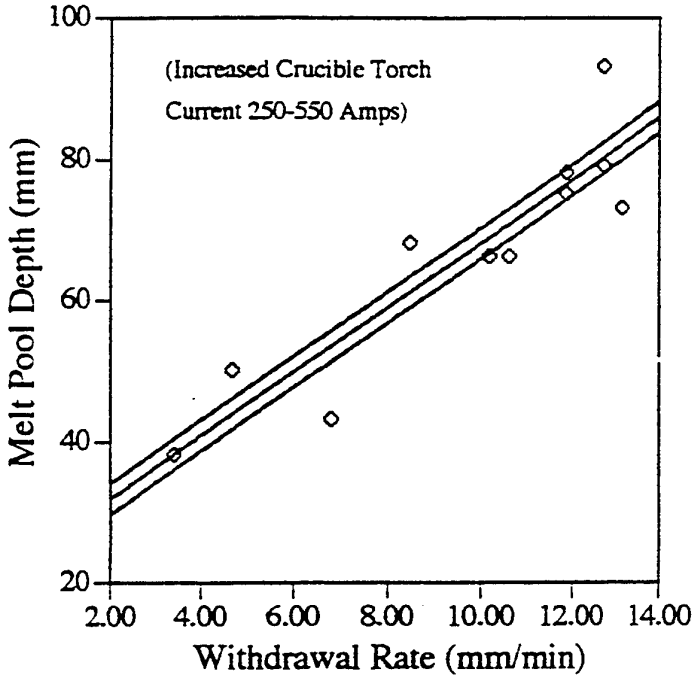

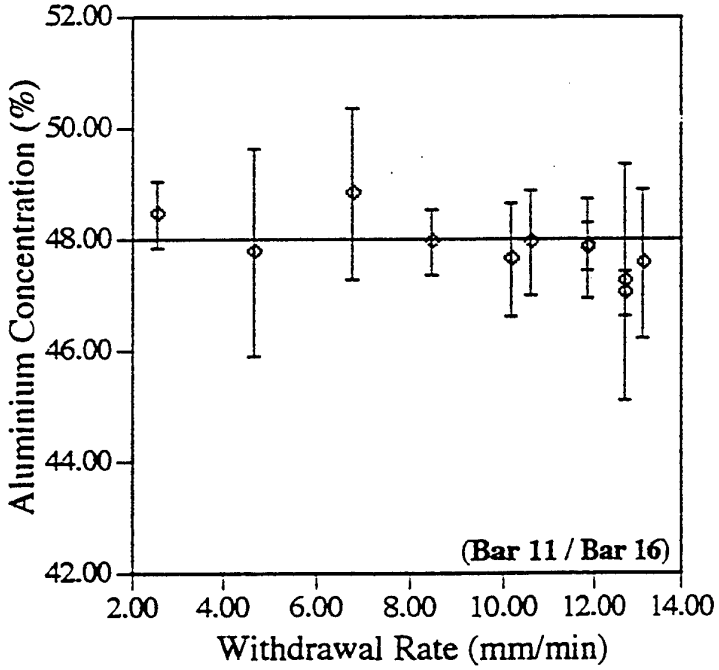

Effect of Ingot Withdrawal Rate on Melt Pool Depth and Al Concentration Variations in PACH Melted Ti-48Al-

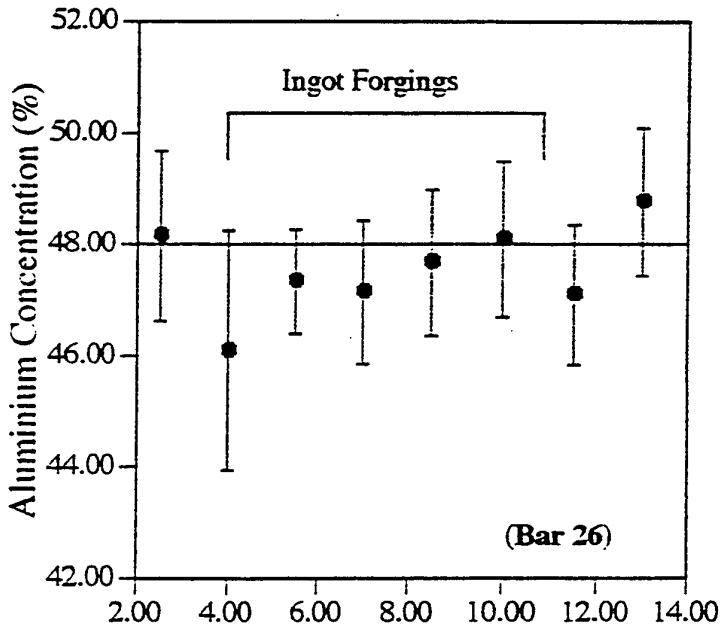

Aluminium Concentration Variations in As-Cast and Isothermally Forged Ti-48Al-2Mn-2Nb

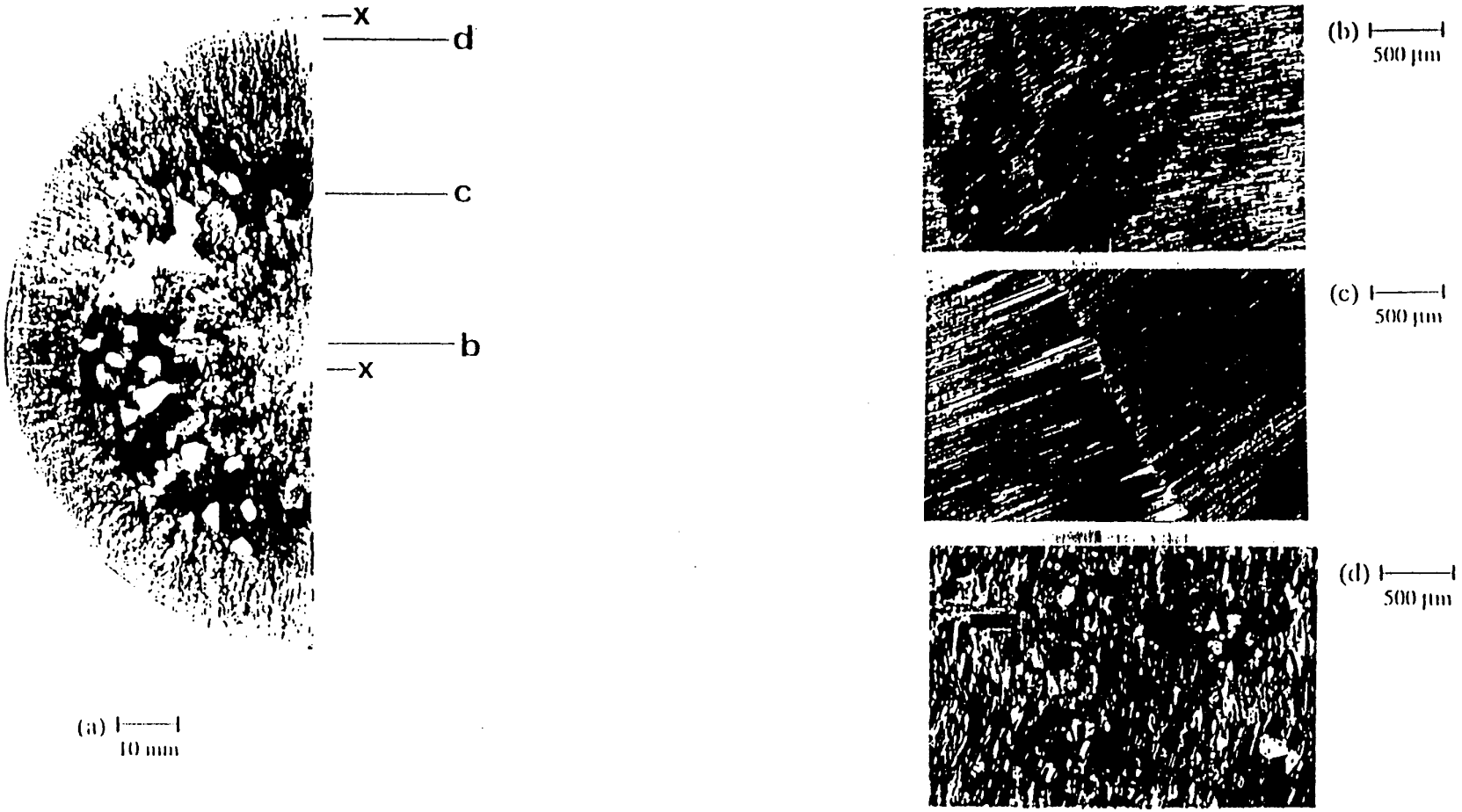

Figure 13 Structure of Billet IF12 at End AA (Prior to Forging)
(Optical)

Microstructural samples taken along section X-X at 90° to plane of macro-section.

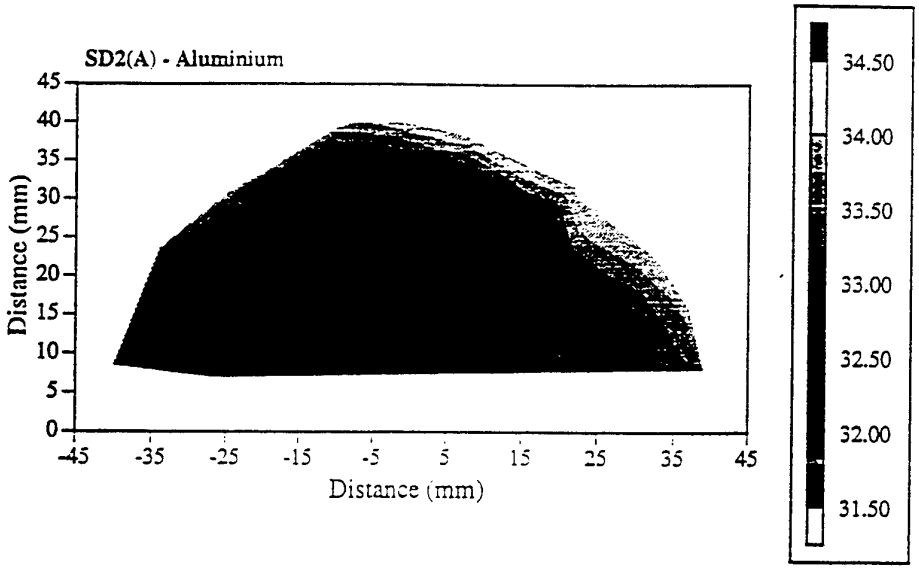
SD2(A) - Aluminium
Distance (mm)
Distance (mm)
45
40
35
30
25
20
15
10
5
0
-45
-35
-25
-15
-5
5
15
25
35
45
34.50
34.00
33.50
33.00
32.50
32.00
31.50

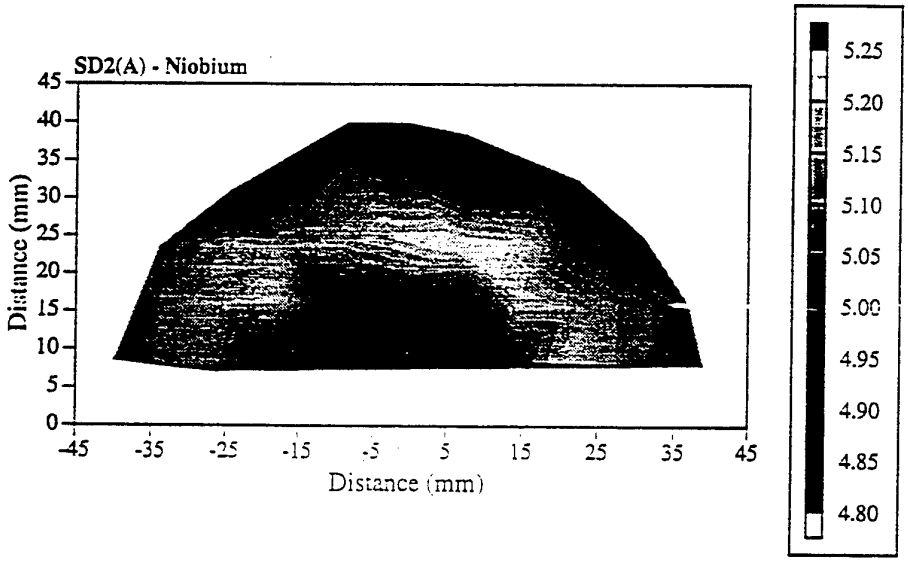
SD2(A) - Niobium
Distance (mm)
Distance (mm)
45
40
35
30
25
20
15
10
5
0
-45
-35
-25
-15
-5
5
15
25
35
45
5.25
5.20
5.15
5.10
5.05
5.00
4.95
4.90
4.85
4.80

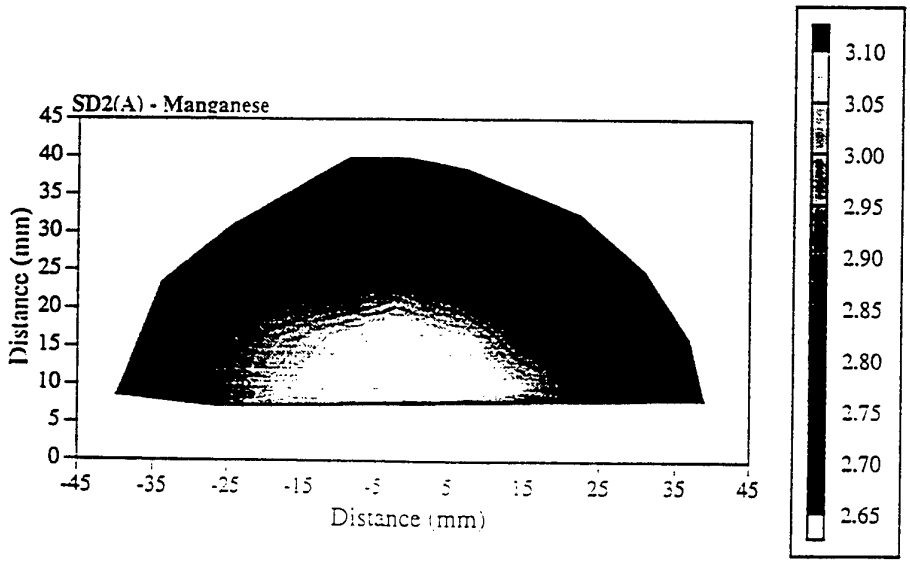
SD2(A) - Manganese
Distance (mm)
Distance (mm)
45
40
35
30
25
20
15
10
5
0
-45
-35
-25
-15
-5
5
15
25
35
45
3.10
3.05
3.00
2.95
2.90
2.85
2.80
2.75
2.70
2.65

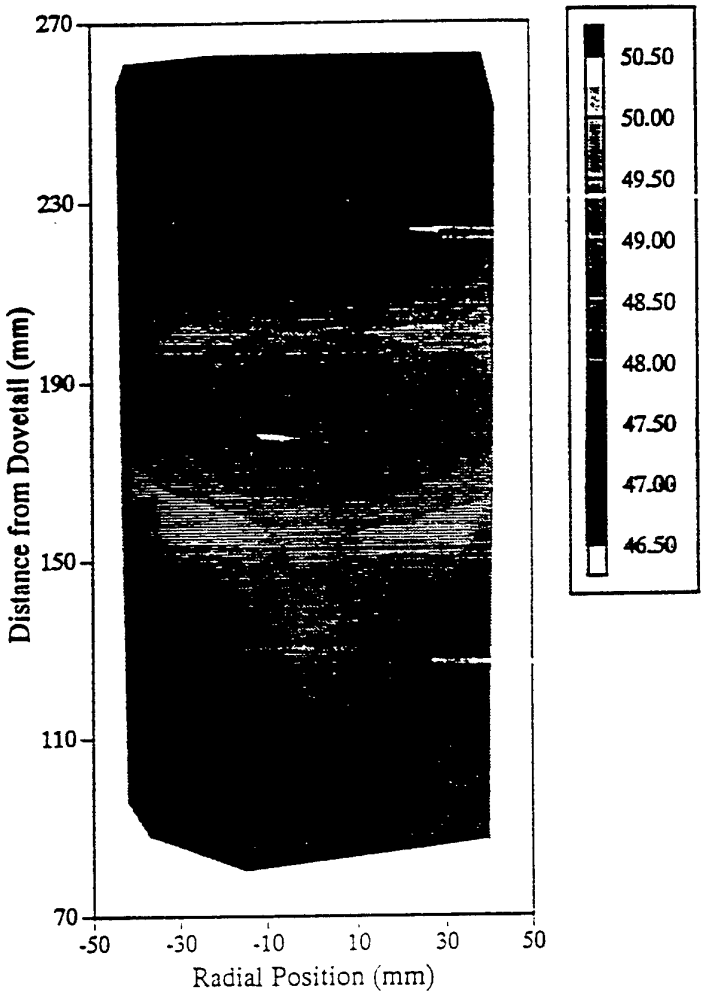

GD-OES Contour Map Showing Longitudinal Variations in Al Concentration as a Function of Distance From Dove-Tail (Ingot Bottom).

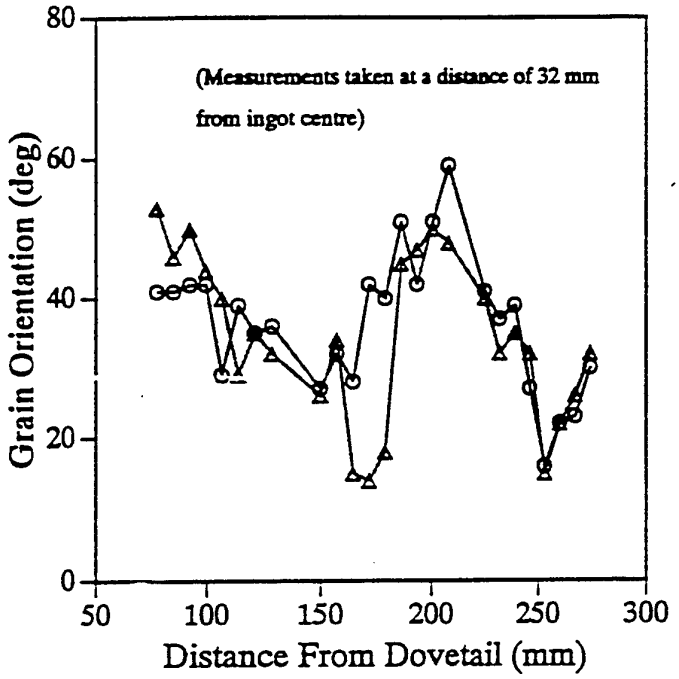

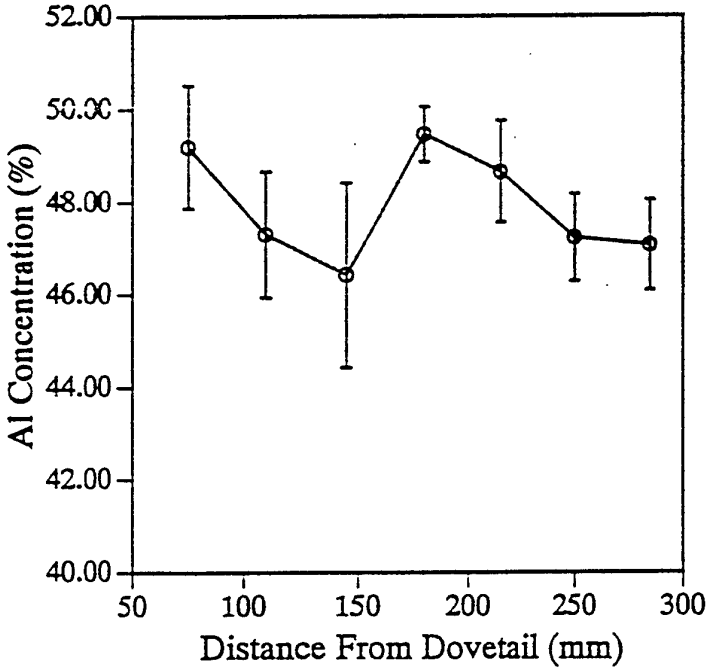

Transient changes in Al concentration and columnar grain orientation with distance from the dovetail.

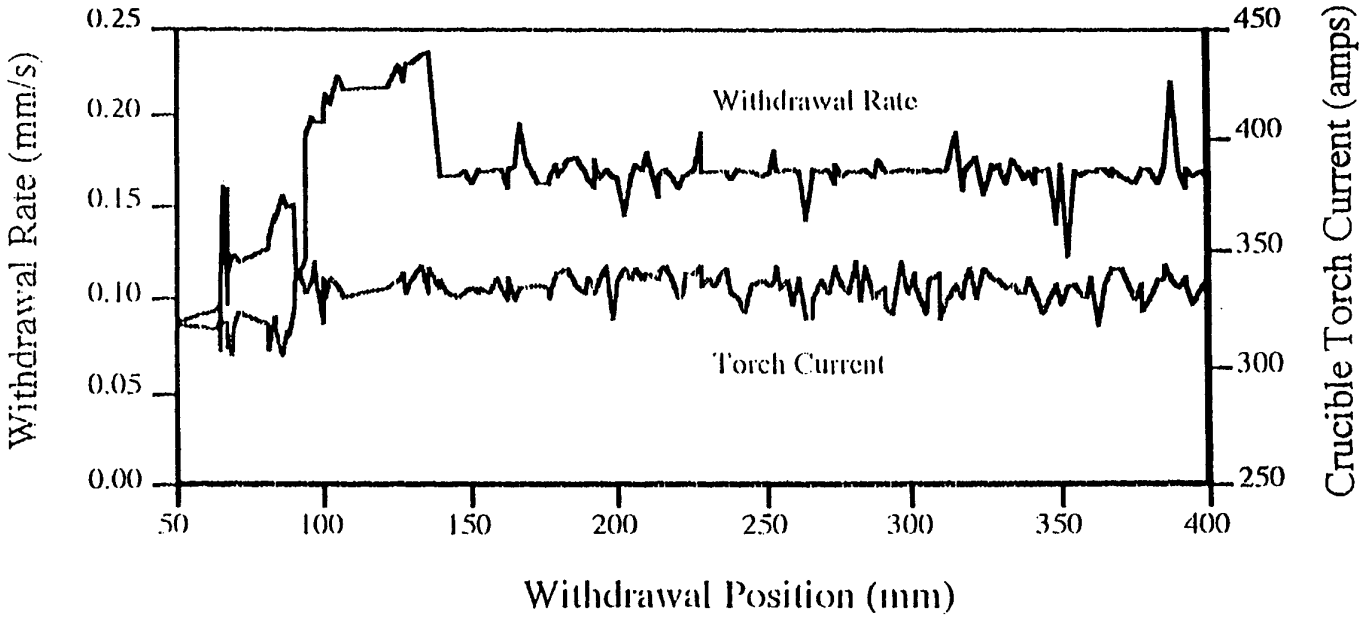

Data acquisition data obtained for Bar 81 showing transient variations in ingot withdrawal conditions within the near-dovetail region (ingot bottom)

Parameters contributing to banding in PACH melted Ti-48Al-2Mn-2Nb:

- Inhomogeneous feed-stock.
- Intermittent pouring of liquid metal from the hearth to the crucible.
- Fluctuations in the height of liquid metal in the crucible.
- Variations in withdrawal rate.
- Changes in the height, pattern and power of the crucible and hearth torches.

Process Monitoring and Control

- Casting rate control through in process monitoring of the level of liquid metal in the crucible and the control of ingot withdrawal and the rate of delivery of the feed-stock to the hearth.

- Temperature distribution within the hearth and crucible through thermal imaging and the associated control of toirch trajectories and operating parameters.

- Optimisation of stir coil design and operational parameters.

Structure of Control System

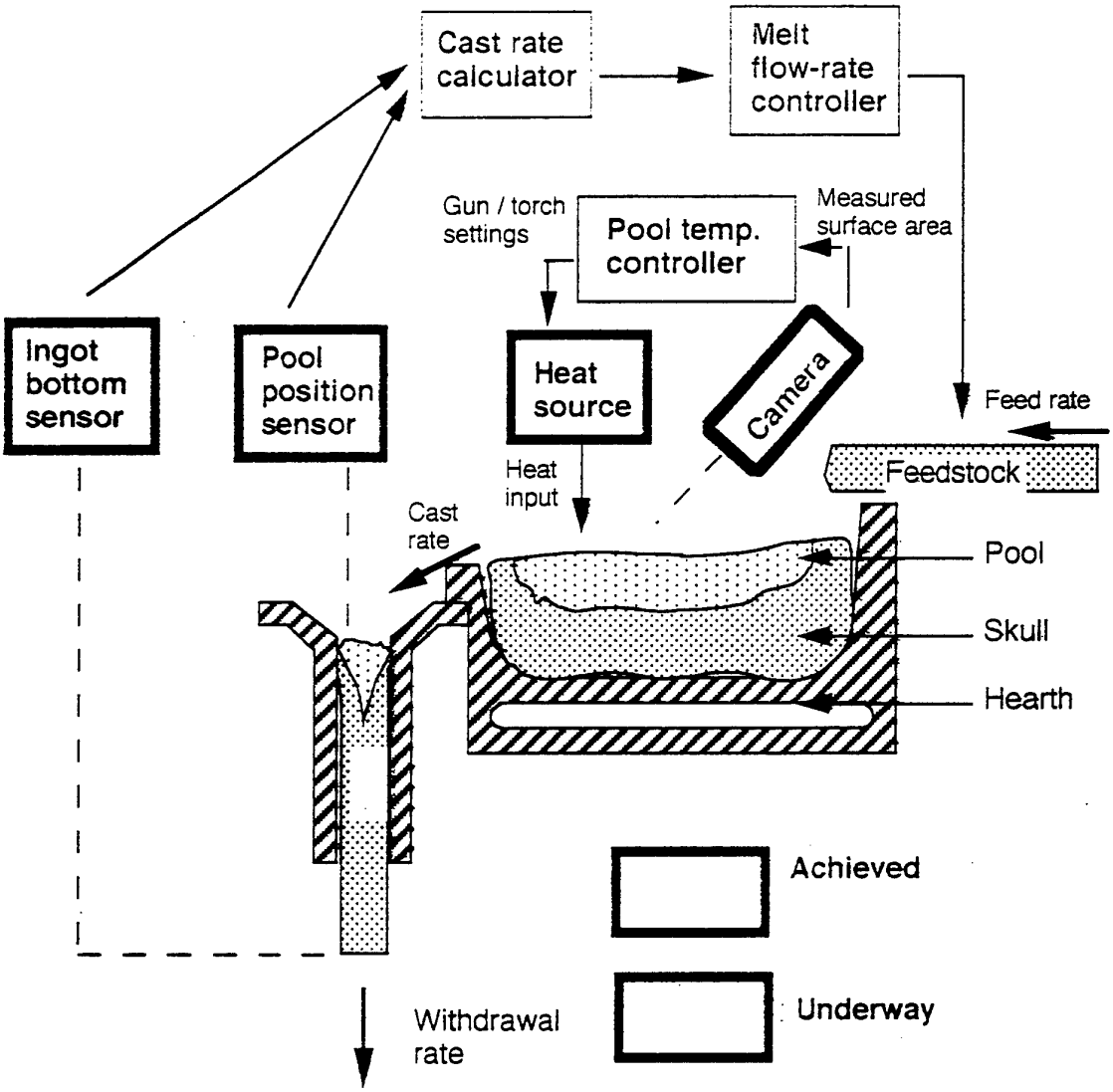

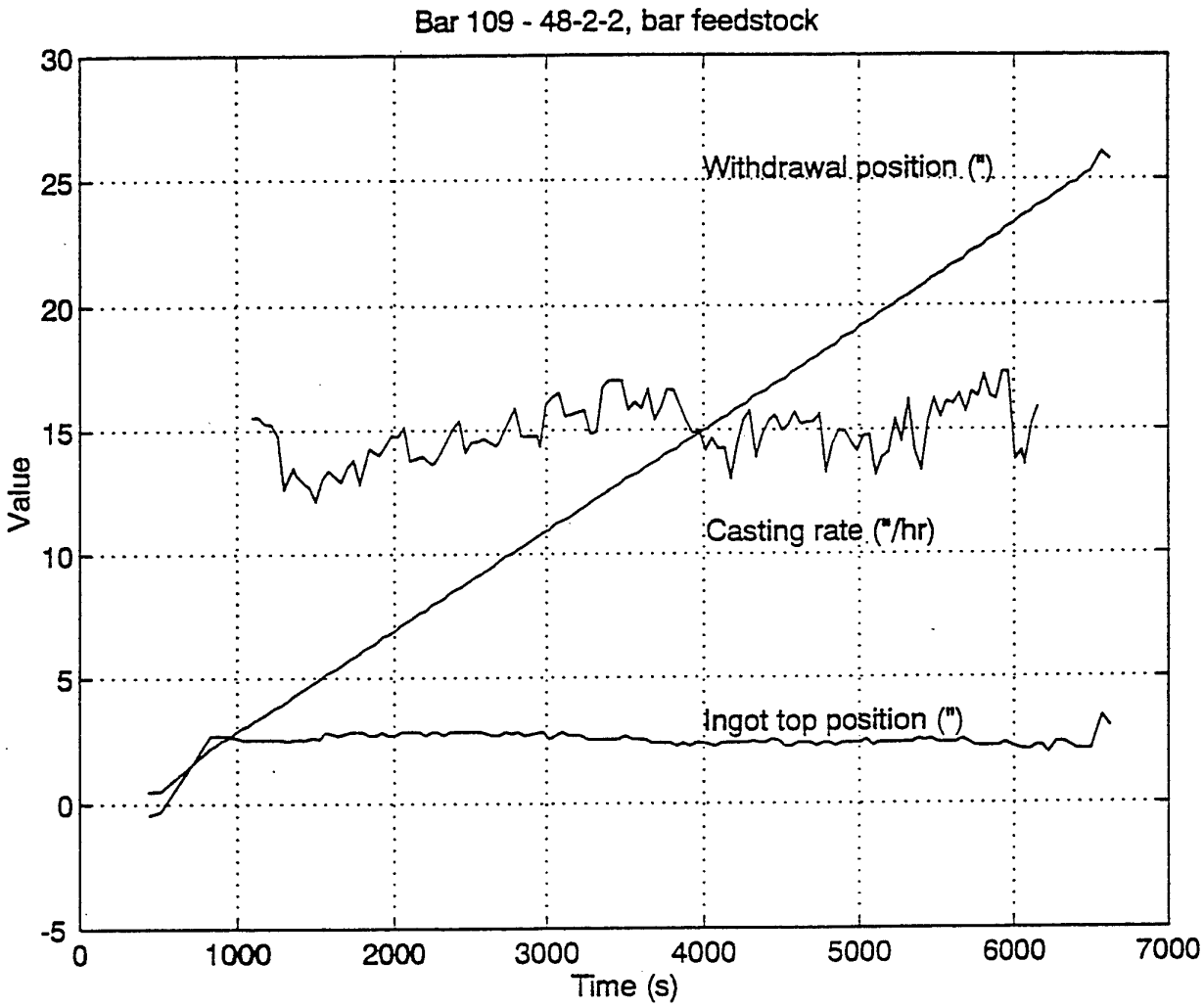
Bar 109 - 48-2-2, bar feedstock
Withdrawal position (")
Casting rate ("/hr)
Ingot top position (")
Value
Time (s)
30
25
20
15
10
5
0
-5
0
1000
2000
3000
4000
5000
6000
7000

Summary of GD-OES Results Showing Effect of Improved Process Control on Aluminium Concentration Variations and Levels of Macro-Segregation

Bar N°	Mean	Max	Min	Range	Std Dev	Comments
11	47.70	50.68	46.42	4.26	0.71	Withdrawal rate & torch current trials. (Compacts, no casting rate control)
16	47.99	49.86	44.70	5.16	0.72	Withdrawal rate & torch current trials. (Compacts, no casting rate control)
26	47.88	49.88	45.26	4.62	0.97	(Compacts, no casting rate control)
81	47.93	50.02	44.42	5.60	1.15	Cast start-up / dove-tail region. (Compacts, no casting rate control)
91	47.93	48.44	46.72	1.73	0.23	Torch current trials. (Bar stock, level detection & casting rate control)
11	48.45	50.52	45.17	5.36	1.09	EDX Micro-Segregation Data. (Inter-Dendritic)
N/A	47.81	51.16	45.28	5.88	0.83	Float Zoned (4.8 -15.0 mm/min). (Interdendritic)

Conclusions

- Despite partition coefficients close to unity ($C/C_0 \approx 0.94 - 1.05$) TiAl based alloys exhibit high levels of inter-dendritic segregation, primarily because of the high Al concentrations.

- GD-OES analysis has shown that these levels of segregation can occur on the macro scale and are often typified by the development of alternating bands of Al enrichment and depletion extending along the length of the ingot. These features are not detected using XRF analysis

- Macrosegregation patterns observed in cast TiAl ingots are retained after forging and have been linked to problems with cracking during forging and changes in heat treatment response during subsequent thermal processing.

- Macrosegregation is found to be most severe in ingots where transient variations in withdrawal rate are at a maximum.